Chem

CellPress
REVIEWS

Review

Alkali Metal Anodes for Rechargeable Batteries

Hua Wang,[1] Dandan Yu,[1] Chengwei Kuang,[1] Liwei Cheng,[1] Wang Li,[1] Xilan Feng,[1] Zheng Zhang,[1] Xinbo Zhang,[2] and Yu Zhang[1,*]

Currently, high-energy rechargeable batteries are being intensively pursued to meet the increasing energy requirements of our modern life and industrial society. Alkali metals are considered some of the most promising anodes for next-generation high-energy batteries because of their superior theoretical specific capacities and low reduction potentials. Here, we provide an overview of the recent development of alkali metal anodes. First, we highlight that their high reactivity, unstable solid electrolyte interphase, dendrite formation, and huge volume change bring great challenges for the safety and lifespan of alkali-metal-based batteries. Then, we summarize various advanced strategies—including the micro- and/or nanostructuring of alkali metals, introduction of stable hosts, structural modification of current collectors, construction of artificial anode-electrolyte interfaces, separator modification, and electrolyte optimization—to address these challenges. Lastly, we present the remaining challenges and possible research directions for further developments.

INTRODUCTION

With the booming development of modern industrial society and looming crisis of fossil fuel availability, the need for rechargeable batteries with high energy density comparable to that of gasoline is becoming increasingly urgent. Commercial Li-ion batteries based on conventional cathodes such as layered-, spinel-, and olivine-type electrode materials are approaching the limits of their capabilities.[1] Because of multi-ion reactions, alkali-metal-free cathodes with high theoretical capacity, including S and O_2, have attracted intense attention (Figure 1A). To pair with these high-capacity cathodes, the pursuit of alkali-metal-containing anodes is becoming a necessity for the development of next-generation high-energy batteries. From this viewpoint, alkali metal anodes have been revived in recent years.

Alkali metal anodes mainly include Li, Na, and K, and their relevant properties are compared and summarized in Table 1.[2–5] Among them, metal Li anode with minimum ionic radius (0.76 Å), density (0.53 g cm^{-3}), redox potential (−3.040 V), and highest theoretical specific capacity (3,860 mAhr g^{-1}) possesses tremendous potential for high-energy-density Li-O_2 and Li-S batteries. Although the theoretical specific capacity and electrochemical potential of metallic Na and K are inferior to those of Li, their high abundance and low cost are still attracting the intense interest of researchers. To date, owing to its high reactivity with electrolyte components, the investigation of plating and stripping behaviors of metallic K has been scarce, so this review mainly focuses on the Li and Na anodes.

When alkali metal anodes are subjected to practical applications, they are confronted with several serious problems in liquid organic electrolyte systems: (1) an

The Bigger Picture

With the increasing demand for green energy and the looming crisis of fossil fuel availability, the development of high-energy batteries comparable to petrol is imperative. The energy density of rechargeable batteries is largely limited by the capacity of electrodes. Hence, alkali-metal-based anodes with high theoretical specific capacity have gained extensive attention. However, the high reactivity of alkali metals leads to inferior performance and safety issues. This review highlights the recent developments in improving the stability of alkali metal anodes to address the above problems. Concrete strategies, including electrode design, interfacial protection, and the optimization of electrolytes, are discussed in detail.

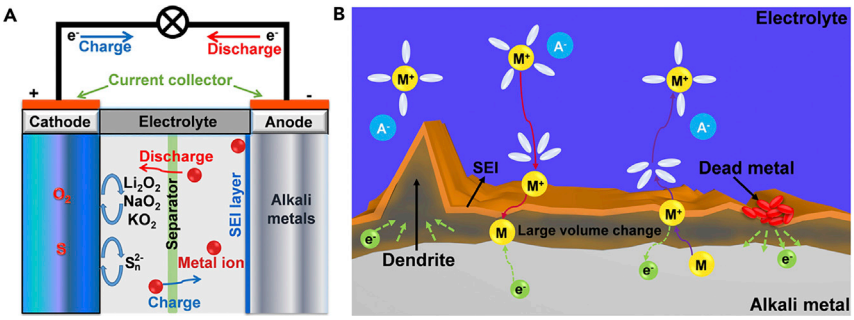

Figure 1. Schematic Illustrations of the Mechanisms and Challenges of AMBs

(A) Schematic of work mechanisms of alkali metal-O_2 and alkali metal-S batteries.

(B) Scheme of reactions between the alkali metal anode and electrolyte in AMBs and challenges of alkali metal anodes.

unstable solid electrolyte interphase (SEI) and low Coulombic efficiency (CE); (2) high reactivity, uneven metallic deposition, and dendritic growth; and (3) large volume changes during plating and stripping cycles (Figure 1B).[6–10] Based on the improved understanding of the formation mechanism of SEI films as well as dendrite nucleation and growth, several effective strategies (such as rational electrode design and interface and electrolyte engineering) have been put into practice and studied in detail.

In this review, we first introduce the main challenges confronting the application of alkali metal anodes, then discuss current strategies that are being used to stabilize alkali metal anodes, and finally offer insights into future developments of alkali-metal-based batteries (AMBs).

CHALLENGES FACING ALKALI METAL ANODES

High Reactivity and Unstable Solid Electrolyte Interphase

Because of their high reactivity, alkali metals exist as compounds and no elemental forms have been found in nature. Alkali metals are extremely sensitive to moisture, and slowly deteriorate even in dry air,[11] bringing considerable technological hindrances for their characterization and application. Furthermore, they tend to spontaneously react with most polar aprotic electrolyte solvents, salt anions, and dissolved cathode materials, leading to undesired cycle performance issues in currently available battery types. In alkali metal-S batteries, the "shuttle effect" derived from polysulfides dissolution induces the corrosion of the alkali metal anode, which results in a severe self-discharge phenomenon, active sulfur loss, and capacity fading upon cycling, while some insoluble and insulating sulfides can accumulate on the surface of alkali metals. Similar to polysulfides, dissolved O_2 on the cathode side in alkali metal-O_2 batteries can diffuse to the anode side and corrode the alkali metal into oxides.

The formation of thin films on electrodes induced by reactions between electrolytes and highly reactive Li was discovered by Dey in 1970, and Peled named it SEI in 1979.[7] Likewise, SEI films can also be formed on Na and K anodes in the initial several cycles. Goodenough and Kim proposed that if the lowest unoccupied molecular orbital (LUMO) of the anode lies above that of the electrolyte, electrons would transfer from the anode to the LUMO of the electrolyte, inducing the reduction of the electrolyte until a passivation SEI layer is created (Figure 2A).[12] The complex SEI film is usually simplified as a dual-layer structure using a mosaic model, and its

[1]School of Chemistry, Beihang University, Beijing 100191, P.R. China

[2]State Key Laboratory of Rare Earth Resource Utilization, Changchun Institute of Applied Chemistry, Chinese Academy of Sciences, Changchun 130022, P.R. China

*Correspondence: jade@buaa.edu.cn

https://doi.org/10.1016/j.chempr.2018.11.005

Table 1. Physical Parameters and Electrochemical Properties of Li-, Na-, and K-Metal Anodes

Alkali Metal	Abundance[a] (wt %)	Atomic Mass	Ionic Radius (A)	Density (g cm^{-3})	Redox Potential[b] (V)	TGSC[c] (mAhr g^{-1})	TVSC[d] (mAhr cm^{-3})	TGED, M-O_2[e] (Whr kg^{-1})	TVED, M-O_2[f] (Whr L^{-1})	TGED, M-S[g] (Whr kg^{-1})	TVED, M-S[h] (Whr L^{-1})
Li	0.0017	6.941	0.76	0.53	−3.04	3,860	2,045	3,456	7,983	2,567	4,261
Na	2.36	22.99	1.02	0.97	−2.71	1,166	1,131	1,602	4,493	1,274	2,370
K	2.09	39.10	1.38	0.86	−2.93	685	589	935	2,001	1,023	1,846

Data are from Wang et al.,[2] Zou et al.,[3] Xiao et al.,[4] and Song et al.[5] The volumetric energy densities were given on the basis of the discharge products (Li_2O_2, Na_2O_2, K_2O and Li_2S, Na_2S, and K_2S) of metal-O_2 and metal-S batteries.

[a]Abundance in Earth's crust.

[b]Redox potential versus standard hydrogen electrode.

[c]Theoretical gravimetric specific capacity.

[d]Theoretical volumetric specific capacity.

[e]Theoretical gravimetric energy density (metal-O_2 batteries).

[f]Theoretical volumetric energy density (metal-O_2 batteries).

[g]Theoretical gravimetric energy density (metal-S batteries).

[h]Theoretical volumetric energy density (metal-S batteries).

components are deeply related to the composition of electrolytes.[15–17] Generally the inner layer of the SEI on Li surface mainly contains inorganic species such as Li_2O, Li_2CO_3, and Li halides, whereas organic polymeric species such as ROCOOLi dominate the outer layer. Specifically, when the organic carbonate such as ethylene carbonate (EC) was used as solvent, Li_2CO_3 and Li ethylene dicarbonate (LEDC) were significant SEI components. Through theoretical calculation, Leung's group believed that these two components were electrochemically stable but thermodynamically unstable.[18] With the reaction barriers lower than 0.92 eV, Li_2CO_3 and LEDC were inclined to be frangible and decompose on Li (100). Because of the decomposition reactions, a thin Li_2O layer was predicted to emerge between Li metal surfaces and the other SEI components, unless Li_2O transformed into LiF during the subsequent reactions. As for ether electrolytes, if $NaPF_6$-glymes were applied for sodium metal battery, the inorganic Na_2O and NaF were the primary constituent of the inner layer while the outer layer was mainly composed of RCH_2ONa.[19]

SEI films act as a barrier to avoid the further decomposition of the electrolyte reduced by alkali metals. Without the protection layer, the reaction between alkali metals and electrolytes goes further, leading to a rapid consumption of alkali metals and electrolytes, which ultimately results in a sharp decline of CE while the repaired SEI exhibits increased thickness with high impedance.[20,21] Meanwhile, the inhomogeneity of the SEI film inevitably leads to an uneven distribution of alkali metal ionic flux, which drives spatial variations in alkali metal deposition during cycling. Furthermore, the localized fracture in the SEI layer caused by volumetric expansion and stress exacerbates the growth of dendrites during the repeating alkali metal plating and stripping cycles because of the locally intensified current density near the cracks. Therefore, it is imperative to maintain the integrity and homogeneity of the SEI film to efficiently protect alkali metal anodes, and a desired SEI film should possess high ionic conductivity and electronic insulating properties to inhibit uneven alkali ion flux, strong mechanical strength to suppress dendrite growth, and high elastic modulus with suitable thickness to accommodate large volume changes.

Dendrite Growth and Large Volume Change

Because of the uneven deposition of alkali metals during the plating and stripping processes, the unexpected dendrite growth exists widely on alkali metal anodes. Even in "alkali-metal-free" cells, anodic dendrite growth can also occur under

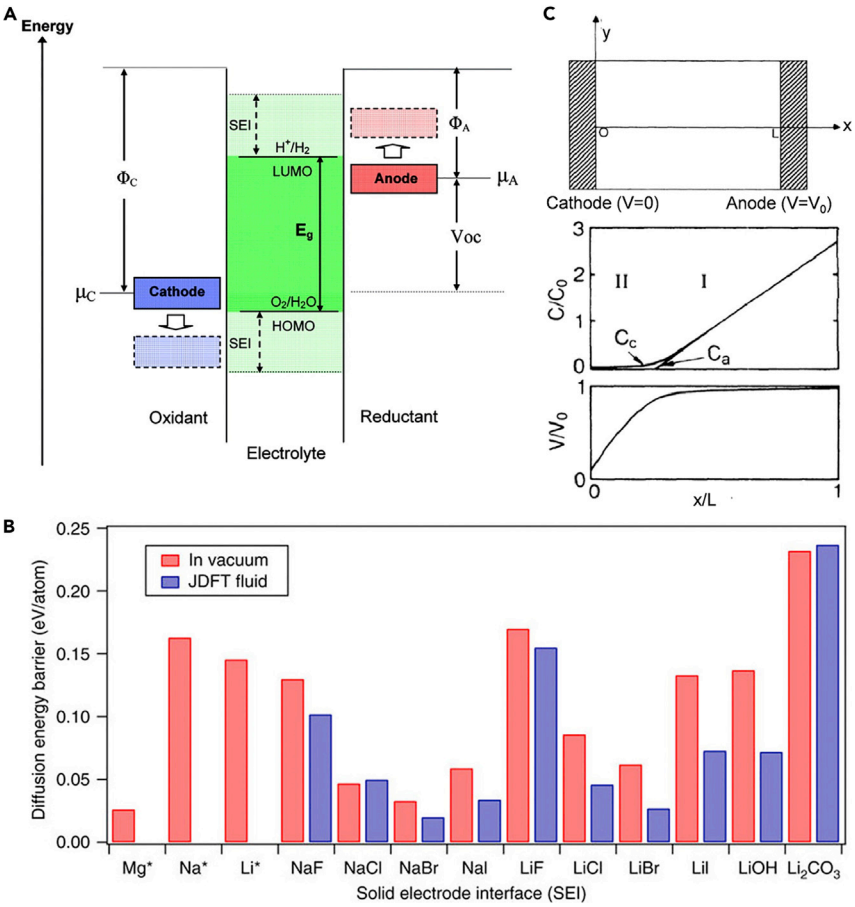

Figure 2. Fundamental Principles of SEI Formation and Schematic of a Space-Charge Model of Li Dendrite Nucleation

(A) Scheme of SEI formation condition in an aqueous electrolyte. Reprinted with permission from Goodenough and Kim.[12] Copyright 2009 American Chemical Society.

(B) Diffusion energy barriers computed for Mg, Na, and Li adatoms on surfaces with possible SEI components. Reprinted with permission from Choudhury et al.[13] Copyright 2017 Springer Nature.

(C) Scheme of the cell (top); profiles of the ion concentrations and electrostatic potential based on theoretical simulation (bottom). Reprinted with permission from Chazalviel.[14] Copyright 1990 American Physical Society.

some conditions, such as high current densities at low temperatures. The dendrites not only cause adverse side reactions but, more seriously, there is a potential risk that they penetrate the separator and reach the cathode, resulting in a short circuit of the working cell, which can cause thermal runaway, burning, and even explosions.[21–23] K is more active than Li and Na and will induce more severe hazards once K dendrites form during battery operation. Thus, preventing undesired dendrite formation is critical for battery safety.

Several models have been proposed to explain the nucleation and growth of dendrites on Li metal. The surface nucleating and diffusion model[24] elucidates that owing to the higher diffusion barrier and weaker interaction between adjacent adatoms, both Li and Na exhibit a tendency to stay isolated rather than agglomerate, and therefore thermodynamically easily grow dendrites. Inspired by the low surface diffusion barrier of Mg, which tends to form a smooth surface, a NaBr (Figure 2B) protective layer on the Na metal largely restricts dendritic Na formation.[13] Chazalviel

proposed an acceptable space-charge model[14,25] to explain Li dendrite behavior. When Li ions are rapidly deposited in dilute salt solutions, anion concentrations near the electrode surface drastically decrease, resulting in a local space-charge region (Figure 2C), and thus the electric field created at the anode-electrolyte interface leads to dendrite growth. The model predicts that dendrites appear at a time very close to Sand's time (τ), which represents the moment when the concentration of cations at the electrode drops to zero.

$$\frac{dC}{dx} = -\frac{Jt_a}{FD},$$

$$J^* = \frac{2FDC_0}{t_a L},$$

$$\tau = \pi D\left(\frac{FC_0}{2Jt_a}\right)^2,$$

where D, F, t_a, C_0, L, and J correspond to the ambipolar diffusion coefficient, Faraday's constant, the anionic transference number, the initial ionic concentration, the distance between electrodes, and the applied current density, respectively. However, this model applies only to high current densities above J^* and cannot explain the observed dendritic growth at low current densities because no Sand behavior is expected in these conditions. Increasing the conductivity and transference number of cations, as well as immobilizing anions, are effective approaches to avoid the generation of space-charge region and thus alleviate dendritic growth. Another widely recognized model states that dendrite growth is self-enhancing. Monroe and Newman[26] thought that the high-curvature tip of dendrites has a fairly intensified electric-field density, which can be preferential sites for alkali-metal-ion deposition, resulting in further growth of dendrites.

Various *in situ* techniques such as transmission electron microscopy (TEM), scanning electron microscopy (SEM), atomic force microscopy (AFM), and nuclear magnetic resonance (NMR) have been employed to understand the processes and mechanisms of alkali metal plating and stripping. *In situ* AFM reveals that the deposition behavior of alkali metals goes through nucleation, growth, dissolution, and detachment processes.[27] The faster dissolution and subsequent detachment of Na dendrites than that of Li dendrites have also been observed in similar electrolytes when the external electrochemical process is halted.[28] In symmetrical cells, the inhomogeneous Li deposition is inclined to occur on the existing dendrites rather than nucleation on other sites, because the SEI film grown on the freshly plated Li possesses fast reaction kinetics,[29] and Na dendrites grow in random directions.[30] The deposited Li and Na microstructures can be quantified by NMR signal intensity at any plating or stripping time.[31,32] Furthermore, current density, temperature,[33] inner pressure of AMBs,[34] and charging capacity also have a significant influence on the dendrite formation. These experiments suggest that fundamental mechanisms related to alkali metal dendrites still demand much more insightful understanding in different circumstances.

In addition to dendrite growth, the large volume change is another fatal factor that can destroy the SEI film on the surface of alkali metal anodes. Such volume changes cause excessive bulk stress in the electrode during the battery operation, which the fragile SEI film cannot withstand, resulting in instability of the internal environment of batteries.[35] Hence, it is of significant importance to develop rational designs that can effectively reduce volume changes of alkali metals during cycling.

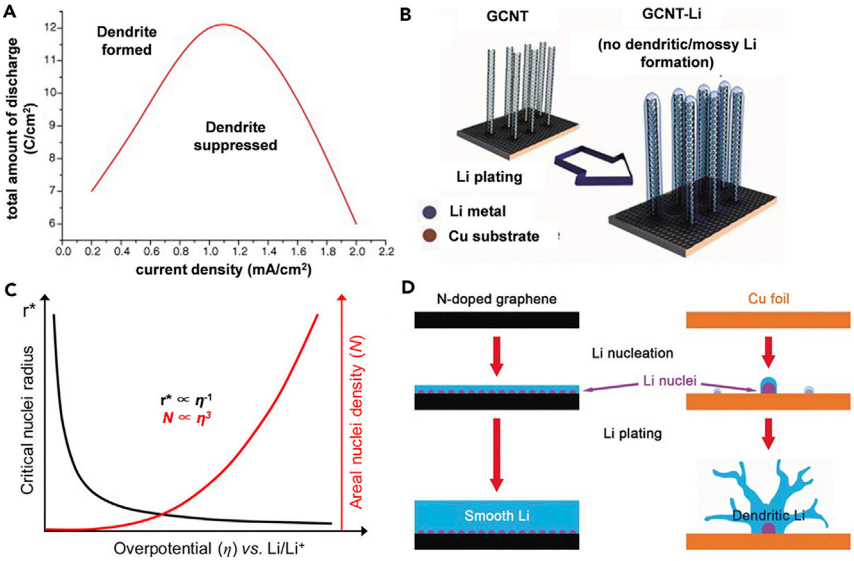

Figure 3. Theoretical Relations Correlated with Dendrite Formation and Schemes of Li-Depositing Behavior on Different Structural Hosts

(A) The empirical critical condition of dendrite formation related to the total amount of discharge and current density. Reprinted from Seong et al.[36]

(B) Scheme of 3D GCNT-Li formation. Reprinted with permission from Raji et al.[38] Copyright 2017 American Chemical Society.

(C) Correlation between critical Li nuclei radius and areal nuclei density corresponding to the overpotential of Li deposition. Reprinted with permission from Pei et al.[39] Copyright 2017 American Chemical Society.

(D) Scheme of Li nucleation and plating processes on N-doped graphene (left) and Cu foils (right). Reprinted with permission from Zhang et al.[40] Copyright 2017 Wiley-VCH Verlag GmbH & Co. KGaA.

STRATEGIES FOR STABILIZING ALKALI METALS

Electrode Design

Micro- and/or Nanostructuring of Alkali Metal Anodes

Generally, alkali metal anodes are present as foils in rechargeable batteries. Surface defects of alkali metal foils can serve as nucleation sites for alkali metal deposition because of topographical and electrical inhomogeneity, further leading to the formation of moss-, dendritic-, or tuber-like structures. Therefore, removing the native layer on pristine alkali metal foils to decrease surface defects can significantly boost the uniformity of alkali metal dissolution and deposition. Moreover, the equation of Sand's time discloses that low current densities play an important role in retarding dendrite growth, and the large surface area of alkali metals can effectively decrease the current density. In this context, micro- and/or nanostructuring of alkali metal anodes has been conducted to increase their surface area. Compared with commercial Li foils, Li particles[36] and Li foils treated by mechanical surface modification[37] exhibit higher surface area and thus effectively suppress dendrite growth. By suitably adjusting the current density or charge capacity, dendrite formation can be inhibited on Li particles (Figure 3A).[36] However, Li particles are easy to detach from current collectors during cycling. For the Li foils treated by surface modification, metallic Li was preferentially deposited in their holes. The plated Li exhibited a dendrite-free morphology even when the current density increased. Nevertheless, as the accumulated Li exceeds the volume of the holes, the subsequent deposited Li will grow out to be dendrites. What's worse, the structures of Li particles and surface-patterned Li foils cannot be preserved for long periods to maintain the performance

of the working battery because of the direct exposure to electrolytes. More efforts should be made to solve this issue. Considering the homogeneous distribution of electrolyte, the highly porous structure is likely to exhibit better performance than its bulk and surface-patterned Li foils.

Stable Hosts for Alkali Metal Anodes

The volume change of the "host-less" alkali metals during plating and stripping cycles is drastic, resulting in poor mechanical stability of the SEI film, low CE, and poor service life of AMBs. The introduction of a stable host is an efficient approach to address the infinite volume variation, and alkali-metal-ion plating and stripping behavior can be regulated to suppress dendrite formation. An ideal deposition matrix should exhibit the following properties: (1) good wettability with alkali metal, (2) high surface area to reduce the local current density, and (3) good compatibility with the electrodes and electrolytes to avoid side reactions.

Alkali metals can be encapsulated in hosts by electrodeposition. Carbon materials such as graphene, carbon nanotubes, graphene-carbon nanotubes (GCNTs), and carbon nanofibers (CNFs) are widely employed as conductive matrices to manipulate alkali metal deposition. Mukherjee et al. found that a porous graphene network (PGN) achieved a maximum specific capacity of 915 mAhr g^{-1} with a CE above 99%, exceeding the theoretical capacity of 372 mAhr g^{-1} to yield LiC_6, which demonstrated that Li was encapsulated within the interior of PGN via defects acting as seeds to initiate Li plating.[41] Compared with the two-dimensional (2D) framework, the 3D structure can provide large surface area and volume to accommodate electrodeposited alkali metals, which can effectively reduce the local current density of the anode, lessening dendrite nucleation and growth rates and therefore minimizing dendrite formation. After prelithiation at 4 mAhr cm^{-2}, the lightweight 3D GCNT (Figure 3B) exhibited a high capacity of 3,351 mAhr g^{-1} and was successfully employed as an anode for the polysulfide- and dendrite-free Li-S battery with alleviated self-discharge performance.[38]

Actually, the final alkali metal plating morphology critically depends on the initial nucleating behavior. Cui and co-workers found that the Li nuclei size was heavily dependent on the electrochemical overpotential and current density, which could be adjusted to suppress dendrite growth at the early stage (Figure 3C).[39] Owing to the different overpotential during Li nucleation, Li ions tended to selectively nucleate on seeds (e.g., Au and Ag) with small nucleation overpotential, and thus Li was guided to uniform deposition without dendrites.[8] Similarly, the functional groups of the N-doped graphene introduced by nitrogen doping offered much more uniform nucleation sites and a smaller nucleation overpotential than the Cu foil and graphene, resulting in suppressed dendritic Li growth at a sprouting stage and smooth Li deposits (Figure 3D).[40]

Thermal infusion is another main method to fabricate the composited alkali metal anode. Electrodeposition easily causes uneven distribution of alkali metals during cycling and inefficient fabrication, while thermal infusion can prestore molten alkali metals inside the host material, preventing utilization of sacrificing cells, which not only predefines the anode space but also supplies an abundant alkali metal source, especially for high-energy-density rechargeable batteries. Graphene, carbon wood, carbon felt, and carbonized metal-organic frameworks (MOFs) serve as hosts to fabricate composite alkali metal anodes by thermal infusion. Graphene-based anodes usually exhibit good flexibility and improved stability against environmental corrosion, in which the original graphene oxide (GO) film can be reduced by molten

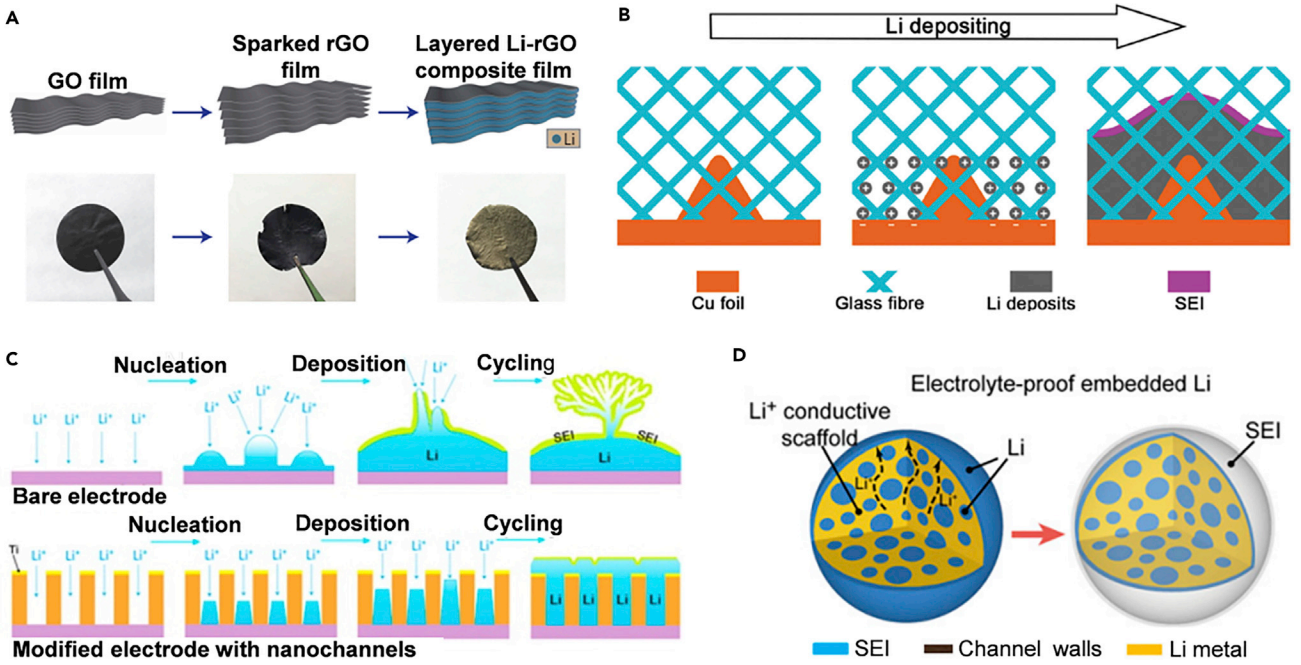

Figure 4. The Design of Stable Hosts to Support and Regulate Li Deposition

(A) Synthetic procedures of a layered Li-rGO composite film and their corresponding digital camera images. Reprinted with permission from Lin et al.[42] Copyright 2016 Springer Nature.

(B) Schematic of Li deposition on 3D GF-modified Cu foils. Reprinted with permission from Cheng et al.[43] Copyright 2016 Wiley-VCH Verlag GmbH & Co. KGaA.

(C) Scheme of the simulation of Li^+ flux during Li deposition over electrodes without (top) and with (bottom) vertical-aligned polyimide nanochannels. Reprinted with permission from Liu et al.[44] Copyright 2016 American Chemical Society.

(D) The SEI film formed on the outer surface of LCNE with embedded Li domains. Reprinted with permission from Lin et al.[45] Copyright 2017 National Academy of Sciences.

Li or Na to yield an expanded reduced GO (rGO) film with a much more porous structure, meanwhile, the capillary force produced by nanogaps facilitated the intrusion of molten alkali metals into rGO interlayers (Figure 4A). This design could minimize the volume change of the composite anode to below 20% during cycling. When charged to 1 V versus Li/Li^+, the Li-rGO electrode showed a specific capacity of 3,390 mAhr g^{-1}.[42] The rGO/Li film with only 5 wt % rGO was successfully employed to construct bending-tolerant anodes for Li-S and Li-O_2 pouch cells with long cycling stability resulting from suppressed electrolyte decomposition, polysulfides, and O_2 corrosion on the surface of rGO/Li.[46] The cycling stability of Na-O_2 and Na/$Na_3V_2(PO_4)_3$ batteries with Na@rGO electrodes was demonstrated to be much better than that of cells with bare Na foils.[47] Some hosts exhibit poor wettability with molten alkali metals, which require a lithiophilic coating such as Si and ZnO to react with molten alkali metals to provide bonding interactions for encapsulation of alkali metals. Inevitably, undesirable impurities are introduced into the Li metal and affect the stability of SEI. Moreover, in most studies both Li and Na metals fill the host without controllable amount during thermal infusion. The excessive Li or Na loading unavoidably decreases the contact area between the electrode and electrolyte. What's worse, dendrite formation might be exacerbated after long cycling. Therefore, the amount of Li or Na infused into different substrates should be optimized, which has a critical effect on the performance and stability of anodes.

The electric-field distribution in the electrolyte can be adjusted by conductive matrices, while the alkali-metal-ion concentration gradient near the anode surface

can be efficiently manipulated by reducing the local current density. Thus, a non-conductive host has been proposed to regulate the concentration distribution in the bulk electrolyte. Because large quantities of polar functional groups serve as the adhesion sites to bind with Li^+ in the electrolyte, insulating polymers such as oxidized polyacrylonitrile nanofibers, 3D glass fibers (Figure 4B),[43] and 3D porous poly-melamine-formaldehyde were coated on Cu foils to guide Li^+ distribution and confine homogeneous Li deposits within the constructed network, although they were not involved in Li deposition. Additionally, a polyimide layer with nanoscale channels vertically coated onto stainless steel was employed to guarantee well-confined Li plating and stripping within the matrix by regulating Li^+ flux and dendrite-free cycling with minimum volume change (Figure 4C).[44]

Nevertheless, most of the composite anodes are limited to current densities below 5 mA cm^{-2}, and capacity fading and instability of electrodes will spring up when the working current density further increases. Fast charging and discharging with current density larger than 10 mA cm^{-2} are usually needed for high-performance rechargeable batteries. 3D frameworks with high ionic conductivity have been designed to alleviate the initial side reactions by protecting the Li surface, minimizing volume change, and realizing a normal operation under ultrahigh current densities. The composite anodes were chemically synthesized by excessive lithiation of inorganic skeletons, in which the obtained matrix can conduct Li^+ and protect the Li metal within the 3D matrix. Uniform Li embedded in a 3D Li_xSi-Li_2O matrix (LCNE) was able to realize safe operation at a high current density up to 10 mA cm^{-2} in symmetric LCNE cells for at least 100 cycles with constant volume and suppressed Li corrosion (Figure 4D).[45] When coupled with the S/CNFs cathode, LCNE-S cells exhibited a lower overpotential compared with conventional Li-S batteries, and had a highly improved capacity of 600 mAhr g^{-1} at a high rate of 2 C.

In short, the matrix plays important roles in alleviating volume change, suppressing dendrite growth, and improving the CE and stability of alkali metal anodes to obtain high energy density. A desired 3D host should possess high surface area, high porosity, and low gravimetric density to regulate the deposition morphology. However, in a non-conductive matrix, Li or Na can be disconnected and lose electric contact easily, while in an electron-conducting matrix the rate performance is restricted by the available electrode-electrolyte interface and sluggish Li^+ or Na^+ diffusion. Considering the pros and cons of non-conductive and electron-conducting hosts, a mixed 3D network should be developed to support alkali metal anodes. Nevertheless, it should be noted that the weight ratio of the host in the composite alkali metal anode should be properly controlled without discounting the high mass and volume energy density of the composite anode.

Modification of Current Collectors

The plating of Li, Na, or K can also occur on the surface of current collectors. However, alkali-metal-ion flux distribution on conventional current collectors with rough surfaces was demonstrated to be inhomogeneous, leading to severe dendrite propagation. Thus, modified current collectors have been developed to accommodate or prestore Li and Na metals. 3D structured current collectors with high surface area are designed to reduce the effective electrode current density and thus suppress dendrite formation. Guo et al. proposed 3D Cu current collectors with a submicron skeleton to regulate Li deposition. Compared with a planar Cu foil, the 3D porous Cu current collector possesses a much larger specific surface area, resulting in a roughly uniform electric field and homogeneous charge distribution (Figure 5A).[48] Hence, a high portion of Li was deposited in the reserved pores of 3D Cu foils without

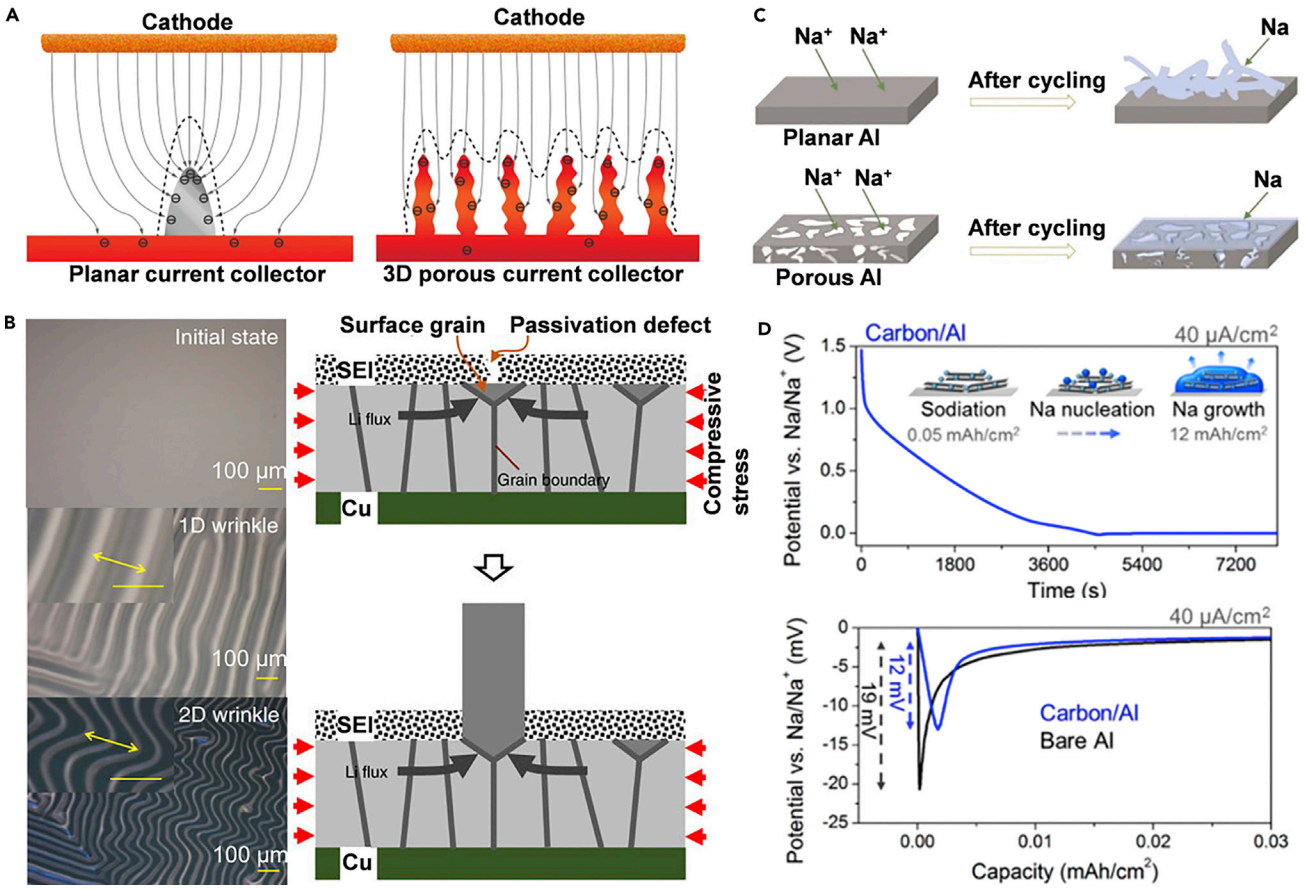

Figure 5. Plating Behaviors of Metallic Li and Na on Modified Current Collectors

(A) Schemes of Li deposition on planar Cu (left) and 3D porous Cu (right) foils, presenting with the electrical field. Reprinted with permission from Yang et al.[48] Copyright 2015 Springer Nature.

(B) Optical microscopy images of the soft Cu/PDMS current collectors during and after Li plating (left); schematic of the stress-driven Li dendrite growth model (right). Reprinted with permission from Wang et al.[34] Copyright 2018 Springer Nature.

(C) Na deposition on planar Al (top) and porous Al (bottom) foils. Reprinted with permission from Liu et al.[9] Copyright 2017 American Chemical Society.

(D) Galvanostatic curve of sodiation and then plating for carbon/Al current collectors (top), as well as sodium nucleation overpotentials (bottom) for bare Al (black curve) and carbon/Al (blue curve) foils. Reprinted with permission from Cohn et al.[49] Copyright 2017 American Chemical Society.

uncontrollable dendrite growth. Furthermore, Wang et al. found that the wrinkles formed on the soft Cu/poly(dimethylsiloxane) (PDMS) substrates evolved from 1D to 2D patterns during Li plating, suggesting the generation of electroplating-induced compressive stress, and proposed a stress-driven Li dendrite growth mechanism (Figure 5B). Consequently, dendrite growth was mitigated on the soft Cu/PDMS substrates through stress relaxation.[34]

In general, Al current collectors cannot be employed as a stable host for the deposition of Li because of the formation of Al-Li alloys during Li plating and stripping processes. Nevertheless, neither Cu nor Al alloys with Na, so both Cu and Al current collectors can be employed to accommodate metallic Na.[9,50] In addition to 3D structured current collectors such as 3D Cu nanowires and honeycomb-like 3D Ni@Cu conductive scaffold, a porous Al foil was proposed by Luo et al. as the plating substrate to mitigate the formation of Na dendrites (Figure 5C).[9] The CE of Na@porous Al electrode was 99.8% over 1,000 cycles at 1.0 mA cm^{-2} with a capacity of 0.5 mAhr cm^{-2}. Employing the Na@porous Al as anode for Na-O_2 cells, the capacity was maintained at about

600 mAhr g^{-1} over 200 cycles although Na deposited was only 1 mAhr cm^{-2}. Carbon black also acted as a nucleation layer on the Al current collectors for *in situ* Na plating.[49] The Na nucleation overpotential could be reduced by coating a carbon layer, which facilitates a smoother Na deposition, and the capacity contributed to sodiation was negligible (Figure 5D). Although the large surface area provided by 3D current collectors and the coated carbon layer could effectively lower local current densities to mitigate dendrite growth, the heavy weight of current collectors inevitably discounts the gravimetric capacity of the alkali metal anode.

Interface Engineering

Artificial SEI Films

Because alkali metals can react with non-aqueous electrolytes, an SEI film can be formed on the surface of alkali metals during initial charge-discharge cycles. However, this film is prone to cracking by large volume changes during prolonged cycling. The restoration of the SEI film intrinsically consumes the alkali metal and electrolyte, leading to a lower CE and shortened lifespan. Hence, constructing a stable and robust film, a so-called artificial SEI, is a significant way to protect alkali metal anodes. The artificial SEI usually has excellent ionic conductivity and low electronic conductivity, guaranteeing that alkali metal deposition takes place underneath.

The electrochemical pretreatment is a promising method to construct an artificial SEI film resembling the SEI layer formed in a working cell. An implantable SEI was constructed on the Li metal anode by electroplating, which effectively suppressed Li dendrite growth. More importantly, the protected Li anode can also work well after being transferred from the original ether-based electrolyte to a carbonate-based electrolyte.[51] Nevertheless, this method is a little complicated for obtaining the protected anode, which includes pretreatment in cells and the subsequent disassembly. *In situ* electropolymerization of ionic liquids was performed to create an ionic polymer membrane on the Na anode to mitigate Na dendrite growth and protect Na from parasitic reactions with the electrolytes, which can be confirmed by the morphology variations of Na anodes at different deposition times (Figure 6A).[30]

Chemical pretreatment is an efficient method to construct the protective layer with desirable components to suppress electrolyte decomposition and dendrite growth. The surface energy and diffusion energy of surface layer significantly influence the Li deposition behavior, which provides theoretical direction for the construction of artificial SEI films to restrain dendrite growth. Zhang's group demonstrated that columnar Li was uniformly deposited on an LiF-rich Cu current collector, because the generated LiF, which possesses low surface diffusion barriers for Li ions, is beneficial for the formation of a stable and homogeneous SEI film that contributes to a well-distributed Li^+ flux.[54] The coatings of alloy/LiCl[55] and Sn[56] on Li or Na anodes are also beneficial to the fast ionic transport. By pretreating Li metal in polyphosphoric acid, an artificial Li_3PO_4 layer was coated on Li metal.[57] Because of the chemical stability in organic electrolytes, high Li^+ conductivity, high Young's modulus around 10–11 GPa, and homogeneous composition of the Li_3PO_4 layer, a uniform Li^+ flux suppressed Li dendrite growth and reduced corrosion of bulk Li was achieved during long-life cycling in Li|$LiFePO_4$ cells. A room-temperature conversion reaction ($4Na + MoS_2 = 2Na_2S + Mo$)[58] was performed to protect Na anodes, whereby Na_2S acts as an artificial SEI film to prevent Na dendrite growth while the 3D host constructed by residual MoS_2 nanosheets largely accommodates the volume change of Na metal.

Atomic layer deposition (ALD) technology, one of physical treatment methods, is utilized to construct the protective layer with controllable thickness and composition

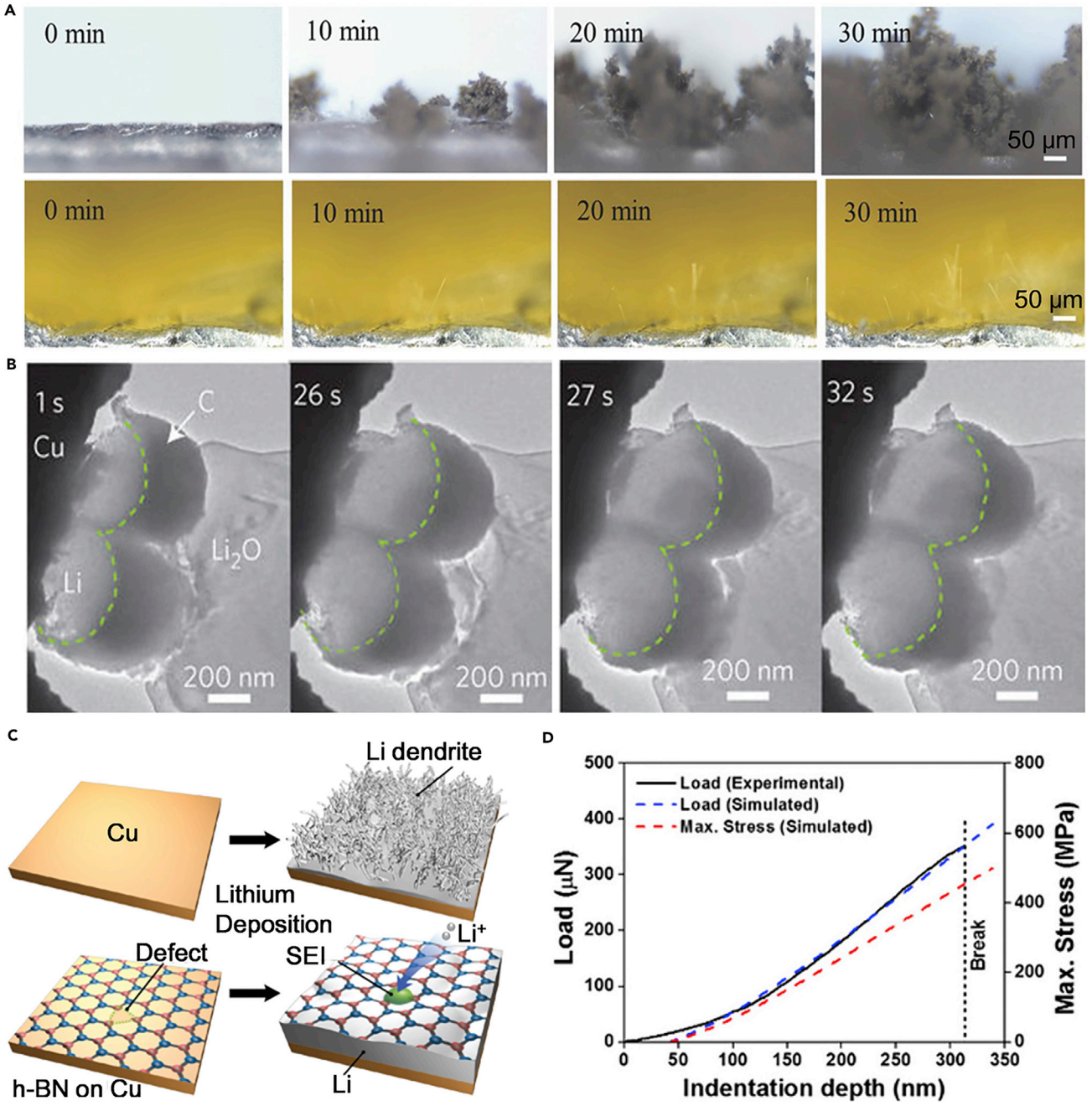

Figure 6. Effects of Artificial SEI Films on Dendrite Growth

(A) *In situ* optical microscopy images of electrochemical Na deposition on the bare Na anode (top) and ionic liquids-membrane-protected Na anode (bottom) taken at different times. Reprinted with permission from Wei et al.[30] Copyright 2017 Wiley-VCH Verlag GmbH & Co. KGaA.

(B) *In situ* TEM images of the Li deposition on hollow carbon nanosphere-decorated Cu wires taken at different times. Reprinted with permission from Zheng et al.[21] Copyright 2014 Springer Nature.

(C) Schematic diagrams of Li deposition on bare Cu foil (top) and the Cu foil covered with an h-BN film (bottom). Reprinted with permission from Yan et al.[52] Copyright 2014 American Chemical Society.

(D) A load-depth curve of the triplet interconnected microspheres until separation. Reprinted with permission from Lee et al.[53] Copyright 2017 American Chemical Society.

for Li and Na anodes. Typically, an Al_2O_3 layer was coated onto Li metal to form a stable and ionically conductive $Li_xAl_2O_3$ alloy after lithiation.[11] The Al_2O_3-protected Li metal showed improved stability against moisture, CO_2, and organic solvents. Compared with bare Li metal, the Li anode protected with 14 nm Al_2O_3 exhibited remarkable stability against sulfur species, resulting in a reduced loss of first cycle capacity and enhanced capacity retention over 100 cycles in Li-S batteries. Considering the low melting point of Na metal (≈98°C), a low-temperature plasma-enhanced process was developed to fabricate Al_2O_3-coated Na anodes whereby no obvious 3D Na dendrite growth was observed after cycling for 450 hr.[59] Considering extra complex steps of these physical methods, Li et al. developed a cost-effective strategy to protect Na and K metal anodes by directly pressing carbon paper on their surface. Compared with pure Na and K metals, sodiated or potassiated carbon possesses less reactive surface, which favors the formation of stable SEI films. Moreover, the large surface area of carbon paper dissipates the current density, homogenizes the ion flux distribution, and mitigates the mossy Na and K deposition.[60]

The artificial SEI films fabricated via chemical/electrochemical pretreatment and ALD are often thin, brittle, and vulnerable to cracking because of volume changes of alkali metal anodes during cycling. The introduction of coating interlayers with high mechanical strength to suppress dendrite growth has aroused wide attention. Zheng et al. designed a protective layer composed of single-layer interconnected amorphous hollow carbon nanospheres.[21] Such a thin carbon layer provided sufficiently high Young's modulus of ~200 GPa to accommodate volume changes. An upward movement of the carbon-sphere thin film was observed by *in situ* TEM, creating free space for Li deposition (Figure 6B). In fact, these low-conductivity carbonaceous coatings serve primarily to add mechanical resistance. Ultrathin 2D graphene and hexagonal boron nitride (h-BN) with point/line defects to allow the penetration of Li^+ are effective layers for the formation of a 2D layer-Li-Cu sandwich structure (Figure 6C), which have a high Young's modulus approaching 1.0 TPa to resist Li dendrites.[52] Moreover, the stability and rate capability of the Na anode were critically dependent on the thickness of the graphene coating layer.[2]

Electronically insulating polymer films are promising protective layers to accommodate the volume change of alkali metals because of their high flexibility. A modified PDMS thin film with nanopores, created by hydrofluoric acid etching, was coated on Cu foils to serve as an artificial layer to improve the cycling stability of Li metal batteries.[61] The nanopores in the PDMS film provide pathways for Li^+ transport. Because of the strong mechanical strength and high flexibility of PDMS, deposited Li is uniformly sandwiched between the PDMS film and Cu foil with the ability to inhibit dendrite growth. Additionally, *in situ* indentation demonstrated that the interconnected microspheres protective layer provided sufficient stress to pressurize the Li dendrites (Figure 6D).[53]

Organic-inorganic hybrid layers are one of the most attractive artificial films, with favorable ionic conductivity and desired flexibility to accommodate the volume changes of alkali metals. Liu et al. proposed a protective layer composed of Cu_3N nanoparticles incorporated into styrene-butadiene rubber (SBR). Cu_3N can react with Li metal to form Li_3N, resulting in good Li^+ conductivity.[62] The elastic modulus of this artificial film is helpful to suppress Li dendrites. In comparison with pure inorganic Li_3N coating, the structural integrity of the hybrid layer was quite stable during Li plating and stripping thanks to the good flexibility of SBR. Moreover, hybrid membranes such as SiO_2@PMMA core-shell nanospheres, Al_2O_3/polyvinylidene

fluoride-hexafluoropropylene (PVdF-HFP) membranes, and alucone are also employed as interfacial layers on alkali metals to alleviate dendrite growth. Therefore, an ideal artificial SEI film should possess high flexibility to accommodate volume changes and a compact structure to impede potential dendrite growth.

Separator Modification

The piercing separator leads to internal short-circuiting along with significant safety hazards. Moreover, the cleavage of the separator caused by puncture by the Li microstructures (e.g., dendrites and fibers) was observed by X-ray tomography.[63] As the separator has a great influence on the alkali-metal-ion diffusion in the bulk electrolyte and dendrite growth, the design of new membranes and the modification of commercial separators have been conducted to resist dendrite growth.

The strong interfacial interaction between the separator and alkali metal can lead to deformation of deposited alkali metals and thus greatly flatten the electrode surface. After polydopamine (PDA) coating, dendrite suppression can be attributed to the well-distributed Li^+ flux, which is facilitated by the enhanced electrolyte uptake capabilities and the strong catecholic adhesion of PDA onto the Li metal surface, which then can relieve the local surface tension of Li metal (Figure 7A).[64] Furthermore, the enhanced separator-electrolyte interaction is beneficial to improving the ionic conductivity of the separator and alkali-metal-ion transference number. Hence, the alkali-metal-ion depletion on the anode surface can be reduced along with retarded dendrite growth. The ZrO_2/polyhedral oligomeric silsesquioxane multilayer deposited on polyethylene (PE) separators can weaken the solvation effect of Li ions.[68] The movement of alkali metal ions can also be increased by using fibrillar polyvinylidene fluoride film, hierarchical chitin fibers, and MOF-coated separator because of the existence of functional groups.

Theoretically, if the shear modulus of the separator is larger than 7 GPa, dendrite suppression can be achieved. Polyoxyzole nanofiber membranes possess dendrite-proof ability arising from an ultimate strength of 525 MPa and Young's modulus of 20 GPa.[69] Additionally, a uniform thermal distribution inside the working battery plays an important role in improving the safety of rechargeable batteries. The BN nanosheets coating layer can decrease the surface area available for the initial Li deposition, so that Li deposits became much larger when using a BN-coated separator (Figure 7B). Owing to very high thermal conductivity, the BN layer can facilitate heat dissipation, leading to a more uniform growth and dissolution of Li.[65] Thanks to the high thermal and mechanical stabilities as well as excellent electrolyte wettability, a poly(vinylidenefluoride-co-hexafluoropropylene)/polyvinylpyrrolidone/antimony oxide (PVdF-HFP/PVP/Sb_2O_3) composite membrane is capable of inhibiting the growth of Li and Na dendrites.[70]

In addition, functional separators have been designed to detect and eliminate dendrites. Separators composed of a polymer-Cu-polymer triple layer were employed to dendrite detection, because a sharp voltage drop between Cu and Li anode could be recorded once dendrites reached the Cu layer but did not penetrate the whole separator (Figure 7C).[66] By introducing SiO_2 nanoparticles[67] or GO film[71] between two polymer membranes, Li dendrites that puncture the separator were eliminated through the chemical reaction with the middle layer (Figure 7D). Bifunctional separators exhibit obvious advantages in alkali metal-S and alkali metal-O_2 batteries because alkali metal anodes are protected from the corrosion of soluble polysulfides and dissolved O_2.[72,73] Although some progress has been made in suppressing dendrite growth by modifying separators, the fundamental mechanism has not

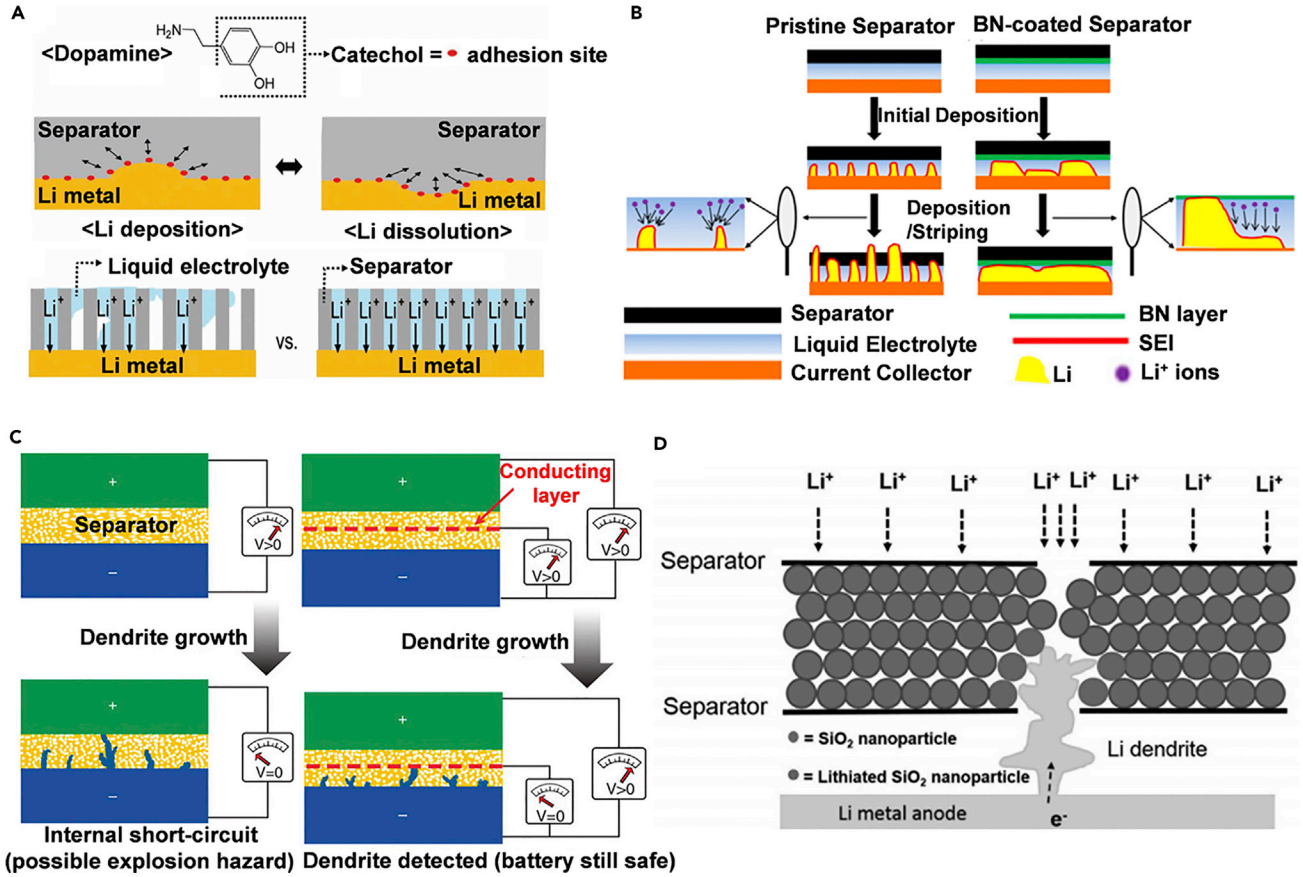

Figure 7. Schemes of Modified Separators in Regulating Li Deposition and Dissolution and Suppressing or Detecting Dendrites

(A) The enhanced adhesion of the PDA-coated PE separator onto Li-metal surface during Li deposition and dissolution (top); the Li-ion flux distribution through the PE and PDA-coated PE separators (bottom). Reprinted with permission from Ryou et al.[64] Copyright 2012 Wiley-VCH Verlag GmbH & Co. KGaA.

(B) Schematic illustrations of Li deposition and striping processes with pristine and BN-coated separators. Reprinted with permission from Luo et al.[65] Copyright 2015 American Chemical Society.

(C) Schematic of dendrite detection in batteries with the traditional separator (left) and polymer-Cu-polymer separator (right). Reprinted with permission from Wu et al.[66] Copyright 2014 Springer Nature.

(D) Proposed mechanism for SiO_2 nanoparticle sandwiched separators to suppress dendrite growth. Reprinted with permission from Liu et al.[67] Copyright 2016 Wiley-VCH Verlag GmbH & Co. KGaA.

been distinctly disclosed owing to the difficulty in studying the behavior of separators in working batteries.

Electrolyte Engineering

Liquid Electrolytes

Because of the low reduction potential of alkali metals, electrolyte components are thermodynamically unstable and decompose into a surface passivation layer on alkali metals. The composition and structure of the *in-situ*-formed SEI film are largely determined by organic solvents, alkali salt types, and additives. A dense and robust SEI film is beneficial to stopping the further reaction between the electrolyte and alkali metal anode, and a uniform interface is helpful to reduce overpotential. Consequently, the regulation of electrolyte components is an efficient approach to stabilize the SEI layer, and some effective strategies including choosing solvents with low reduction potential, enhancing the concentrations of salts, and introducing proper functional additives have been proposed.

According to Goodenough's perspective about the relationship between the SEI formation and LUMO/highest occupied molecular orbital (HOMO) of electrolyte, selecting the solvent with low reduction potential is an effective way to solve the problems of electrolyte decomposition. Carbonate solvents can be easily reduced to form undesirable organic components in SEI films because of their high reduction potentials. However, ether-based electrolytes have attracted attention because of their lower reduction potentials, and taking 1,2-dimethoxyethane (DME) as an example, it has the lowest potential of −1.68 V (versus Li^+/Li) among the liner ethers, implying the low possibility of direct reactions between DME and Li metal. Zhang et al. found that needle-like Li dendrites were generated in propylene carbonate (PC)-based electrolytes with different Li salts, while nodule-like Li depositions with a smaller surface area and round edges were present in DME-based electrolytes, suggesting that ether-based electrolytes were much more stable in the presence of Li metal.[74] Cui et al. successfully realized the highly reversible room-temperature Na plating and stripping by using $NaPF_6$ in diglyme, but failed when employing $NaPF_6$ in carbonate solvents (Figure 8A).[19] The utilization of $NaPF_6$ enables the generation of an SEI film including inorganic Na_2O and NaF with high impenetrability to electrolyte solvents and high shear moduli, which promotes a well-distributed Na^+ flux and suppresses the dendritic growth of Na deposits.

Salt concentration affects the stabilization and cycling efficiency of alkali metal anodes. Except for the decreased conductivity, concentrated electrolytes usually exhibit high ionic transference number, reduced reactivity, and enhanced electrochemical and thermal stabilities. The equation of Sand's time discloses τ that increases with the initial metal-ion concentration, demonstrating that an increase in alkali ion concentration can retard dendrite formation. Moreover, a high number of alkali metal ions in the electrolyte lead to a unique coordination structure. As a consequence, the number of uncoordinated solvent molecules decreases, which mitigates alkali metal surface corrosion. For example, the Li ions are usually solvated with four or five solvent molecules in the liquid electrolyte,[77] and Xu et al. proved that the desolvation process of Li^+ is the major energy-consuming step during the "ion transfer" through the SEI film.[78] The solvation and desolvation of Li^+ depend on the solvent species and Li^+ concentration.[78,79] In low-salt-concentration electrolytes, a large Li^+ solvation shell forms, leading to relatively lower mobility of solvated Li^+ cations. However, an concentrated electrolyte comprising 7 M $LiN(SO_2CF_3)_2$ (LiTFSI) in 1,3-dioxolane/DME (1:1, v/v) delivered a high Li^+ transference number (t_{Li+}) of 0.73, indicating that this Li salt was more capable of transporting Li^+.[80] The high t_{Li+} is beneficial for a sufficient Li^+ flux and rapid Li^+ transfer between the electrolyte and Li anode. As a mass of anion balances the cation (Li^+) and anion ($TFSI^-$) in the vicinity of the Li anode, no excess Li^+ is available for the formation of Li dendrites. Moreover, the high viscosity of electrolytes with ultrahigh salt concentrations provides an additional chemical pressure to inhibit Li dendrite growth. Consequently, the Li-S battery that use this highly concentrated electrolyte exhibited a reversible capacity of 770 mAhr g^{-1} with capacity retention of 74% after 100 cycles at 0.2 C, and the CE reached nearly 100% after the first cycle. Besides, Xiao et al. found that high potassium bis(fluorosulfonyl)imide (KFSI)-DME electrolyte was beneficial for the passivation of K surface and K^+ conduction, and a stable SEI was established in the early stages, which is proved by overpotential unchanged within 200 cycles. However, 1 M potassium hexafluorophosphate (KPF_6)-DME, 1 M potassium bis(trifluorosulfonyl)imide-DME, and 0.8 M KPF_6 in EC/diethyl carbonate resulted in irreversible K deposition and dissolution with rapid capacity decay (Figure 8B).[4] DME molecules in high-salt electrolyte donate their oxygen lone-pair electrons to K^+ (solvation) and have lower HOMO, which mitigated the oxidative

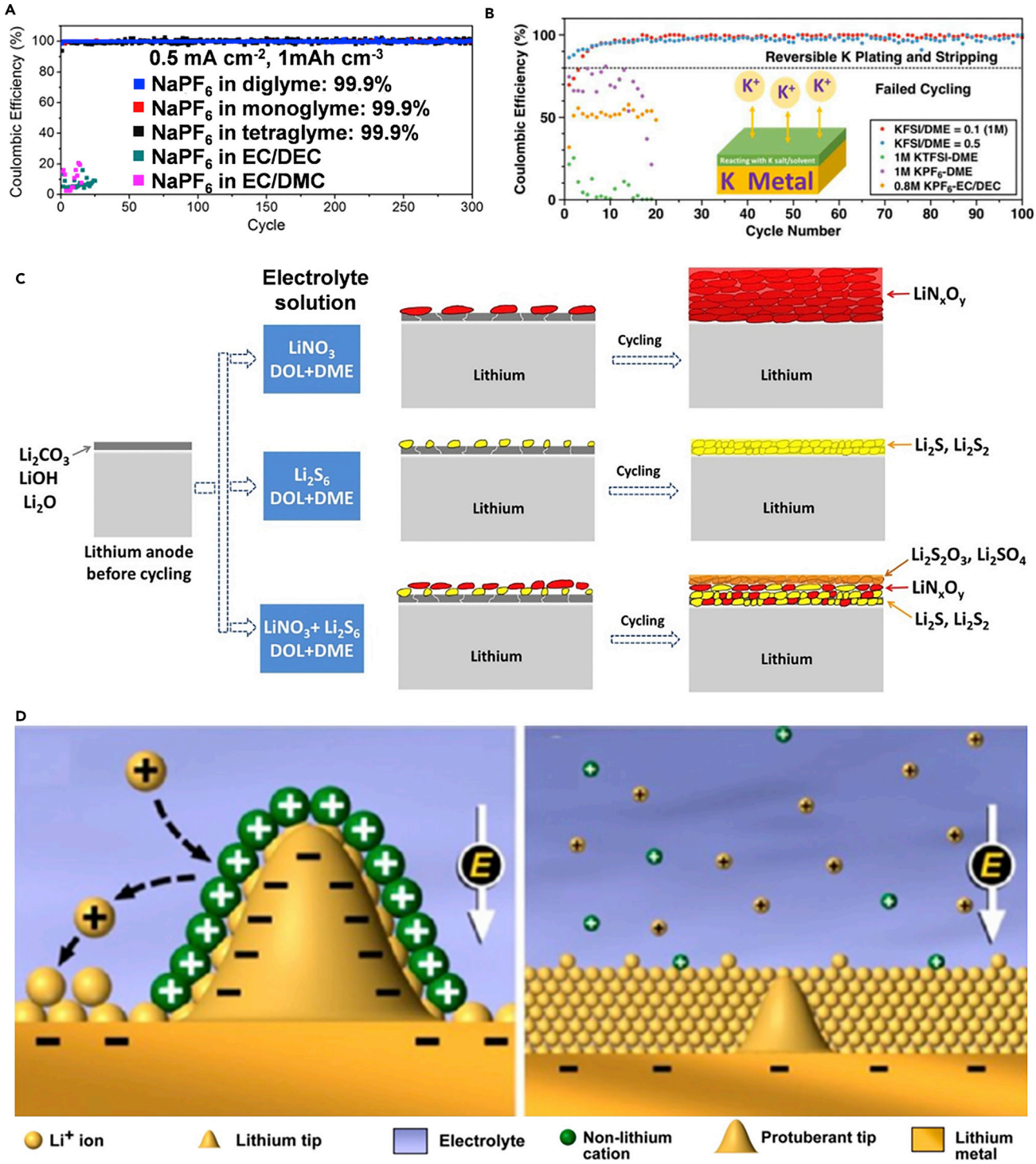

Figure 8. Optimizing Liquid Electrolytes by Adjusting Components and Introducing Additives

(A) CEs of Na/Cu coin cells cycled with 1 M $NaPF_6$ in different solvents. Reprinted with permission from Seh et al.[19] Copyright 2015 American Chemical Society.

(B) CEs of K/Cu coin cells with various electrolyte formulations. Reprinted with permission from Xiao et al.[4] Copyright 2017 American Chemical Society.

(C) SEI films formed on Li anodes of Li-S cells with different electrolyte additives. Reprinted from Xiong et al.[75]

(D) Self-healing electrostatic shield mechanism of Li deposits. Reprinted with permission from Ding et al.[76] Copyright 2013 American Chemical Society.

decomposition. Therefore, the wide electrochemical window is up to 5 V versus K/K^+ in the highly concentrated KFSI-DME electrolyte, which can be coupled with high-voltage cathodes. K/potassium Prussian blue cells displayed an average discharge capacity of 65 mAhr g^{-1} over 50 cycles with a high CE of 98% at 100 mA g^{-1}. Recently, considering the high cost and poor ionic conductivity of high-concentration electrolytes (HCE), localized HCE by diluting an HCE with an "inert" diluent has been reported.[81] The diluent is required to exhibit an electrochemical stability window similar to that of the HCE and does not dissolve the salt but is miscible with the solvent, and the Li^+-solvent solvates in the HCE. This method, based on diluting high concentrations of electrolytes without the dissolution of salts, opens a new way for electrolyte design.

An ideal electrolyte additive should react with alkali metals prior to electrolyte and form a strong, uniform, and chemically stable SEI layer. Generally speaking, LiF with extremely large band gap of 13.6 eV is a good candidate as an SEI component.[13,82] Fluoroethylene carbonate (FEC) with a very low LUMO level of −0.87 eV is easy to reduce on the surface of Li metal anode to form a dense and mechanically strong LiF-rich SEI layer, which is beneficial to suppressing dendrite growth.[83] For example, Zhang et al. introduced FEC and $LiNO_3$ into DME electrolyte to alter the Li solvation sheath and formed LiF and LiN_xO_y SEI films.[84] A 30 mol % LiF additive in a 1 M LiTFSI/PC electrolyte enabled the development of a conformal crystalline SEI film, leading to smooth Li deposition without dendrites and 25-fold enhancement in the lifetime of symmetric Li/Li cells.[85] Similarly, an electrolyte comprising 1 M LiF_3SO_3 in tetraethylene glycol dimethyl ether-FEC (5:1, v/v) was beneficial for the formation of a protective film on the Li metal surface, which effectively protected the Li metal from corrosion under attack by dissolved O_2 and organic solvents. As a result, the Li-O_2 battery with this FEC-containing electrolyte showed a much more stable cycling performance, with a fixed capacity of 1,000 mAhr g^{-1} at 300 mA g^{-1} after 100 cycles.[86] Nevertheless, FEC is not a panacea additive for the construction of reliable Na metal batteries, because of the sudden onset of polarization during discharge resulting in inefficient Na plating and stripping.[87] In addition, Guo's group found that FEC could aggravate the electrolyte decomposition in a symmetric K foil cell, which severely affects the uniformity and stability of the SEI layer, indicating that FEC is not a good choice for K-ion batteries.[88]

Moreover, $LiNO_3$ is the most commonly used additive for Li-S batteries and can be reduced to yield insoluble LiN_xO_y that protects Li metal from further reactions with polysulfides. Because of the synergetic effects of $LiNO_3$ and Li_2S_n (n = 4–8), a smooth and stable SEI film can be produced on Li metal (Figure 8C).[75] Li et al. demonstrated that Li dendrite growth was effectively suppressed by controlling the concentrations of Li_2S_8 and $LiNO_3$.[89] Contrary to the previous findings in the Li metal anode system, Wang et al. proved that Na_2S_6-$NaNO_3$ as co-additives into 1 M $NaPF_6$ in diglyme had an adverse effect on Na anode owing to the fact that Na metal could preferentially react with $NaNO_3$.[90] However, when using Na_2S_6 as additives into 1 M $NaPF_6$ in diglyme, the SEI films composed of Na_2O, Na_2S_2, and Na_2S were robust enough to protect the Na surface from further reacting with the electrolyte components. The Na_2S_6-treated Na/S cell exhibited much more cycling stability than the untreated Na/S cell, indicating the passivation of Na anodes and the alleviated shuttle effect of Na-S batteries. Unfortunately, a majority of additives are continuously consumed during repetitive restoration of SEI films because they are sacrificed to prevent exhaustion of alkali metal anodes, solvents, or salt anions in the subsequent cycles.

On the basis of a self-healing electrostatic shield mechanism, Xu's group demonstrated that low concentrations of Rb^+ or Cs^+, which have a lower reduction potential

than Li^+, can form a positively charged electrostatic shield around the initial Li protuberance.[76] Owing to the repulsive interaction between Li^+ and non-Li cations, Li^+ will be deposited to adjacent regions of the anode until a smooth deposition layer forms (Figure 8D). Even when testing Li metal with pre-existing dendrites, the needle-like Li protrusions were transformed into smaller spherical particles after contacting with 1 M $LiPF_6$/PC with 0.05 M $CsPF_6$ additive. Obviously, whether alkali metals can be plated preferentially depends on the concentration of deposition additives. Similarly, an ionic liquid additive, namely, 1-dodecyl-1-methylpyrrolidinium ($Pyr1(12)^+$) bis(fluorosulfonyl)imide (FSI^-), could suppress Li dendrite growth by the synergistic effect of cations and anions. The $Pyr1(12)^+$ cations not only can engage an electrostatic shielding effect but can also add a "lithiophobic" effect via the non-polar aliphatic chain attached to the pyrrolidinium, whereas the FSI^- anions can induce the formation of rigid SEI layers.[91] Consequently, developing new multifunctional additives to improve the stability of SEI films and regulate the distribution of alkali metal ions may be one of the significant trends for AMBs.

Solid-State Electrolytes

Solid-state electrolytes (SSEs) possess several prominent advantages such as easy encapsulation, non-inflammability, high chemical and electrochemical stability, and high mechanical strength, which make it a good choice for the large-scale application of AMBs. In general, the ionic conductivity of SSEs is still much lower than that of liquid electrolytes at room temperature.

Inorganic SSEs are promising candidates for preventing alkali metal dendrite penetration by way of their unity ionic transfer number and strong mechanical strength, although unstable electrode-electrolyte interface, high interface resistance, and poor stability in air hinder their practical demonstration. Owing to the difference in ionic conductivity at grain boundaries (GBs), dendrite growth along GBs where the electric field was enhanced locally during charge was found even by *in situ* SEM observation in some oxide-type and sulfide-based SSEs,[92–95] while initial dendrite formation was mostly ascribed to the inhomogeneous contact between SSEs and alkali metal anodes.[93,96] An ultrathin Al_2O_3 coating was introduced to boost the Li wettability of $Li_7La_{2.75}Ca_{0.25}Zr_{1.75}Nb_{0.25}O_{12}$ (LLCZN) by forming Li-Al-O alloys at the Li-electrolyte interface (Figure 9A), leading to significantly decreased total impedance of symmetric Li/Li cells.[97] Lithiophilic materials such as Al, Au, Si, ZnO, and Ge were also employed to improve the interfacial contact between the oxide-garnet-type electrolyte and Li anode by alloying. Moreover, the *in situ*-formed Na^+-conductive layer on the surface of 380°C heat-treated $Na_3Zr_2(PO_4)(SiO_4)_2$ (H-NASICON) was capable of achieving better wetting and adhesion across the Na-H-NASICON interface with lower interfacial resistance and suppressed dendrite growth (Figure 9B).[96] Compared with inorganic SSEs, solid polymer electrolytes (SPEs) possess good processability, high flexibility, and strengthened resistance to volume changes of alkali metals during cycling. Polyethylene oxide (PEO)-based electrolytes are one of the most promising SPEs because of their high solubility for alkali salts and high chain flexibility that can mechanically mitigate dendritic growth. However, PEO hosts that imbibe organic electrolytes usually suffer from several problems such as low room-temperature ionic conductivity, poor dimensional stability, and uncontrollable dendrite growth of alkali metals at high temperatures. Crosslinking polymers play an important role in improving dimensional stability and suppressing the crystallization of PEO at room temperature. Khurana et al. designed a Li-ion conducting SPE composed of stiff semi-crystalline PE chains covalently crosslinked by PEO segments.[100] High conductivity ($>10^{-4}$ S cm^{-1} at 25°C) could be obtained by tuning the PE backbone length

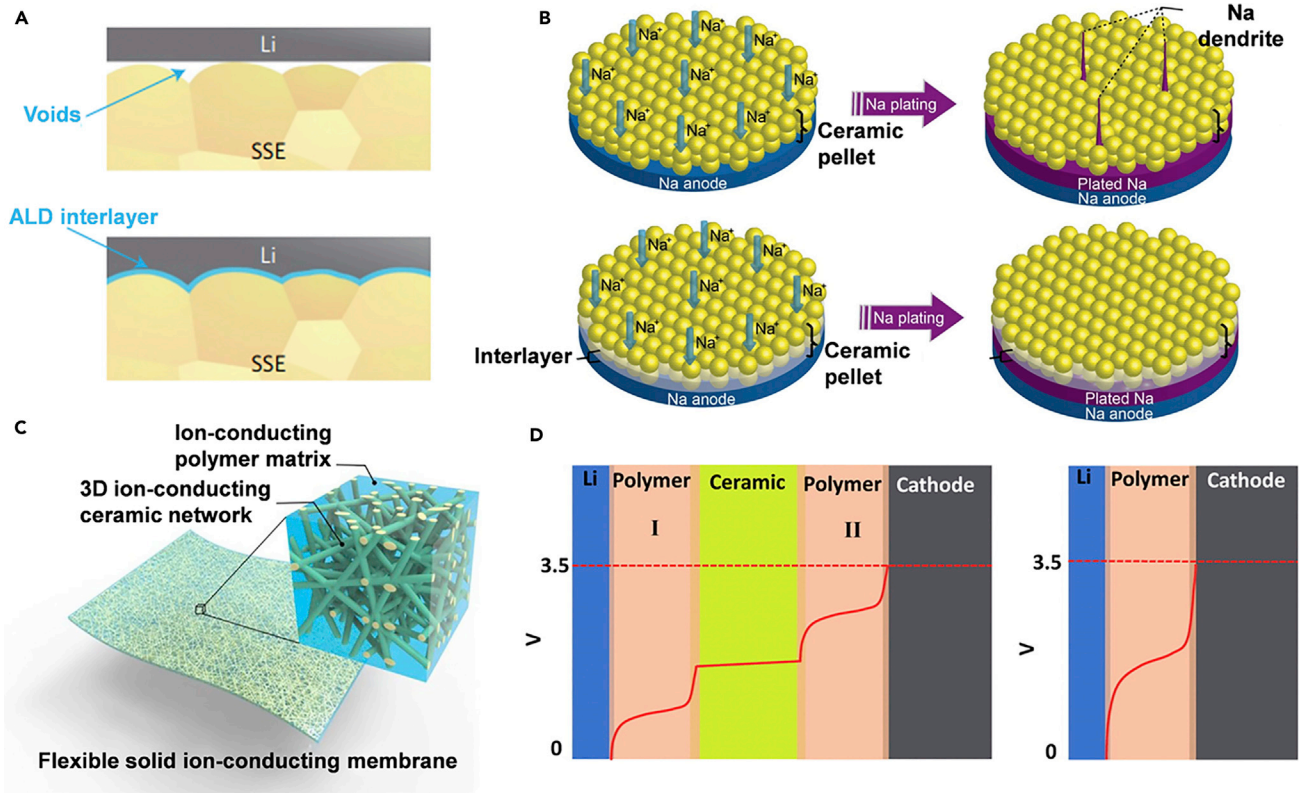

Figure 9. Schematic Illustrations of Solid-State Electrolytes for Li- and Na-Metal Batteries

(A) The contact interface between LLCZN and Li metal without (top) and with (bottom) ALD Al_2O_3. Reprinted with permission from Han et al.[97] Copyright 2016 Springer Nature.

(B) Na plating behavior on the NASICON-pellet-Na-metal interface without (top) and with (bottom) a Na^+ conductive layer. Reprinted with permission from Zhou et al.[96] Copyright 2017 American Chemical Society.

(C) Scheme of the 3D garnet fiber-reinforced CPL. Reprinted with permission from Fu et al.[98] Copyright 2016 National Academy of Sciences.

(D) Electric potential profiles across the PCPSE (left) and single polymer electrolyte (right) in the charged cell. Reprinted with permission from Zhou et al.[99] Copyright 2016 American Chemical Society.

between crosslinks and the PEO segment lengths. More importantly, although possessing low shear modulus, this crosslinked SPE still exhibited remarkable dendrite resistance, indicating that a high modulus ($G' > 2\ G_{Li}$) is not a requirement for SPEs to control dendrite proliferation.

Inorganic compounds such as SiO_2, garnet-type materials, and Na^+ conductors (NASICON) have been integrated with polymer matrices to fabricate composite polymer electrolytes (CPLs) with favorable ionic conductivity, high mechanical flexibility, and high modulus. The nanosized inorganic particles in the CPLs can significantly decrease the crystallinity of polymers and increase contact area with the polymer electrolyte, which results in high ionic conductivity. Lin et al. demonstrated that a PEO-based composite electrolyte dispersed with *in-situ*-synthesized SiO_2 nanospheres inside exhibited an improved Li^+ conductivity of 1.2×10^{-3} S cm^{-1} at 60°C.[101] Additionally, the content ratio of the inorganic filler also has a great influence on the ionic conductivity of CPLs. With the addition of 40 wt % NASICON-type $Na_{3.4}Zr_{1.8}Mg_{0.2}Si_2PO_{12}$ filler, the Na^+ conductivity of the CPL increased from 9.0×10^{-4} to 2.4×10^{-3} S cm^{-1} at 80°C while the polarization voltage of the Na/CPLs/$Na_3V_2(PO_4)_3$ cell decreased from 0.16 to 0.06 V at 0.1 C.[102] To avoid the agglomeration of individual nanoparticles, nanowire- or

nanofiber-based 3D networks were introduced into the polymer matrices to improve the ionic conductivity by providing more ionic transport pathways. By infiltrating a LiTFSI-PEO polymer into a 3D porous garnet-type $Li_{6.4}La_3Zr_2Al_{0.2}O_{12}$ nanofiber network, flexible and ion-conducting hybrid membranes were fabricated (Figure 9C).[98] Thanks to the good mechanical support provided by the 3D network, this composite electrolyte exhibited high thermal stability and fire-retardant properties. The symmetric Li/CPL/Li cell showed a long cyclability at 0.5 mA cm^{-2}, indicating its good mechanical stability that can block Li dendrites. However, most of the CPLs still need to work at high temperature. To satisfy the application demand of the low-melting-point Na metal, a liquid plasticizer (1-ethyl-3-methylimidazolium bis(fluorosulfonyl)) was further incorporated into the PEO-$NaClO_4$-SiO_2 matrix to improve room-temperature ionic conductivity of the hybrid electrolyte.[103]

It was found that the Sand's time varies inversely proportional to t_{anion} (transference number of anion), suggesting that alkali metal ionic transference number has a vital impact on dendrite growth. Combining the merits of inorganic and polymeric electrolytes, Goodenough et al. designed a polymer/ceramic/polymer sandwich electrolyte (PCPSE), where the oligoethylene oxide pendants attached on the cross-linked poly(ethylene glycol) methyl ether acrylate facilitate Li^+ transfer and the irreversible reduction of the $Li_{1.3}Al_{0.3}Ti_{1.7}(PO_4)_3$ (LATP) was prevented by the isolating effect of polymer layers. In comparison with single-polymer electrolytes in the batteries, the prepared PCPSE effectively reduced the electric-field intensity across the interface and stabilized the polymer electrolyte without decomposition (Figure 9D).[99] Moreover, the good wetting of the polymer to Li anode resulted in lower Li^+ transfer resistance and a more uniform Li^+ flux across the interface, thus suppressing the dendrite formation on the GBs of LATP. Similarly, both $Li_7La_3Zr_2O_{12}$ and $Na_3Zr_2(PO_4)$ $(SiO_4)_2$ containing PCPSEs also exhibited superior stability and dendritic inhibition.

Although SSEs exhibit better safety than liquid electrolytes in rechargeable batteries, the room-temperature ionic conductivity, stability against alkali metals, and intimate electrode-electrolyte contact interface need to be further enhanced for their practical application in AMBs.

CONCLUSION AND PERSPECTIVE

Alkali metals (Li, Na, and K) are ideal anode materials for high-energy rechargeable batteries such as the alkali-S and alkali-O_2 cells. Unfortunately, their high reactivity, large volume change, dendrite growth, unstable SEI films, and low CE during charge-discharge cycling have largely hampered the practical application of alkali metal anodes for rechargeable batteries. With a deeper understanding of the formation of SEI films as well as dendrite nucleation and growth, significant progress in electrode design, interfacial protection, and the optimization of electrolytes has been made to address these challenges. Nevertheless, these strategies have their own advantages and disadvantages (Table 2) and are usually effective under certain conditions, but how to integrate the individual solution into a rechargeable battery with a long lifespan at high current densities and high CE remains to be solved. Both the theoretical and experimental investigations of AMBs need to be intensified to meet the demands for commercialization.

Many challenges and possible development directions for future AMBs research include the following. (1) For evaluating the ability to suppress dendrite growth

Table 2. The Advantages and Disadvantages of Different Strategies for Addressing the Challenges Confronted by Alkali Metal Anodes

Classification	Methods		Advantages	Disadvantages
Electrode design	micro- and/or nanostructuring of alkali metal anodes		effectively decrease the current density	difficulty in maintaining the micro- and/or nanostructures of alkali metal anodes after cycling
	stable hosts for alkali metal anodes		possess the abilities to accommodate alkali metals and mitigate volume changes; regulation of electric-field distribution or alkali-metal-ion concentration gradient to suppress dendrite growth	need an additional predeposition process to load alkali metals
	modification of current collectors		reduce the current density; manipulate alkali metal deposition sites; provide room for alkali metal depositions; alleviate the volume change during cycling	heavyweight discount gravimetric capacity of composited alkali metal anodes; easy oxidation of the deposited alkali metals
Interface engineering	artificial SEI films		stabilize the alkali metal surface and mitigate dendrite growth	poor mechanical stability of most protection layers
	separator modification		improve battery safety; regulate alkali-metal-ion flux distribution or suppress the initiation of dendrite growth	narrow range of structure design
Electrolyte engineering	liquid electrolytes	high concentrations	delay the start time for dendrite formation	high cost
		electrolyte additives	stabilize and adjust the properties of SEI films with minimum side reactions	continuous consumption of sacrificial additives during repetitive restoration of SEI films; strict concentration dependence of deposition additives
	solid-state electrolytes	inorganic solid electrolytes	high mechanical strength	low ionic conductivities at room temperature; brittleness; processing difficulties; high cost; poor wettability and stability toward alkali metals
		solid polymer electrolytes	ease of processing; low cost; high flexibility; good wettability with electrodes; strengthened resistance to volume changes of alkali metals	poor ionic conductivities at room temperature; narrow operating temperature; weak mechanical stability
		composited polymer electrolytes	cost-effectiveness and enhanced mechanical strength	low ionic conductivities at room temperature; high interface resistance

and the stability of SEI films, *in situ* characterization techniques for alkali metal anodes need to be developed urgently to reveal their original fine morphologies, components, and structures, which can provide more reliable information than *ex situ* techniques. (2) The low CE of alkali metal anodes is always ignored in the reported research, because the oversufficient alkali metal conceals the capacity loss of alkali metals in each dissolution-deposition cycle although dendrite suppression is achieved. Therefore, the simultaneous inhibition of dendrite growth and substantial improvement of CE should attract enough attention to realize the extensive utilization of alkali metal anodes in AMBs. (3) The complexation of alkali metal ions with an appropriate agent that can increase the electrochemical polarization of alkali metal deposition and seeking ideal additives that can be adsorbed onto protuberances of alkali metal surface to regulate the ionic distribution should be efficient ways to retard the corresponding alkali metal deposition. (4) Universally accepted criteria to evaluate alkali metal anodes, such as the choice of tested cell pattern (coin or pouch cells) and the definition of high current densities, should be established. (5) Because of the ultrahigh reactivity of metallic K, the research on K metal batteries is still in the infant stage, and far behind that of Li- and Na-based batteries. Thus, increased efforts should be undertaken for the advancement of K metal batteries. Effective strategies to stabilize Li and Na herald a new dawn for K metal anodes. (6) Exploring non-dendritic alkali metal anodes such as a liquid K-Na alloy for dendrite-free metallic K batteries should be a promising strategy for realizing the application of AMBs. (7) Being capable of adjusting current densities, alleviating volume change, and eliminating dendrite growth, a universal, lightweight, and low-cost micro- and/or nanostructured matrix is critically needed to support alkali metals. (8) The stability, ionic conductivity, and mechanical strength of SEI films are determined by their composition and structure. The SEI layer with low energy barriers for alkali-metal-ion diffusion contributes to stable and homogeneous deposition. Chemical reactions between the alkali metal anode and electrolyte, which greatly facilitate the selection of organic solvents, alkali salts, and electrolyte additives, need to be deeply investigated. (9) Although SSEs usually exhibit a high ionic conductivity at high temperatures, the room-temperature ionic conductivity of SSEs needs to be further enhanced. Moreover, optimization of the contact between SSEs and electrodes is required to decrease interfacial resistance.

Despite being confronted with many obstacles, the wide application of high-energy-density AMBs is of great significance, and much more efforts should be made in fundamental study, material design, and advanced characterization techniques to facilitate their advancement toward practical applications.

ACKNOWLEDGMENTS

The authors acknowledge the financial support of the National Natural Science Foundation of China (51822201 and 51502009) and the 111 Project (B14009).

AUTHOR CONTRIBUTIONS

Y.Z. proposed the topic of the review. H.W. investigated the literature and wrote the Introduction. H.W. and L.C. wrote the section Challenges Facing Alkali Metal Anodes. D.Y. wrote the sections Electrode Design and Liquid Electrolytes. W.L. wrote the Artificial SEI Films section. X.F. wrote the Separator Modification section. C.K. wrote the Solid-State Electrolytes section. Z.Z. revised the figures. X.Z. wrote the Conclusion and Perspective. H.W. and D.Y. revised a draft of the review. All the authors discussed and revised the manuscript.

REFERENCES AND NOTES

1. Guo, Y., Li, H., and Zhai, T. (2017). Reviving lithium-metal anodes for next-generation high-energy batteries. Adv. Mater. *29*, 1700007.

2. Wang, H., Wang, C., Matios, E., and Li, W. (2017). Critical role of ultrathin graphene films with tunable thickness in enabling highly stable sodium metal anodes. Nano Lett. *17*, 6808–6815.

3. Zou, X., Xiong, P., Zhao, J., Hu, J., Liu, Z., and Xu, Y. (2017). Recent research progress in non-aqueous potassium-ion batteries. Phys. Chem. Chem. Phys. *19*, 26495–26506.

4. Xiao, N., McCulloch, W.D., and Wu, Y. (2017). Reversible dendrite-free potassium plating and stripping electrochemistry for potassium secondary batteries. J. Am. Chem. Soc. *139*, 9475–9478.

5. Song, K., Agyeman, D.A., Park, M., Yang, J., and Kang, Y. (2017). High-energy-density metal-oxygen batteries: lithium-oxygen batteries vs sodium-oxygen batteries. Adv. Mater. *29*, 1606572.

6. Lin, D., Liu, Y., and Cui, Y. (2017). Reviving the lithium metal anode for high-energy batteries. Nat. Nanotechnol. *12*, 194–206.

7. Cheng, X.B., Zhang, R., Zhao, C.Z., and Zhang, Q. (2017). Toward safe lithium metal anode in rechargeable batteries. Chem. Rev. *117*, 10403–10473.

8. Yan, K., Lu, Z., Lee, H.-W., Xiong, F., Hsu, P.-C., Li, Y., Zhao, J., Chu, S., and Cui, Y. (2016). Selective deposition and stable encapsulation of lithium through heterogeneous seeded growth. Nat. Energy *1*, 16010.

9. Liu, S., Tang, S., Zhang, X., Wang, A., Yang, Q.H., and Luo, J. (2017). Porous Al current collector for dendrite-free Na metal anodes. Nano Lett. *17*, 5862–5868.

10. Ye, H., Xin, S., Yin, Y.X., Li, J.Y., Guo, Y.G., and Wan, L.J. (2017). Stable Li plating/stripping electrochemistry realized by a hybrid Li reservoir in spherical carbon granules with 3D conducting skeletons. J. Am. Chem. Soc. *139*, 5916–5922.

11. Kozen, A.C., Lin, C.-F., Pearse, A.J., Schroeder, M.A., Han, X., Hu, L., Lee, S.-B., Rubloff, G.W., and Noked, M. (2015). Next-generation lithium metal anode engineering *via* atomic layer deposition. ACS Nano *9*, 5884–5892.

12. Goodenough, J.B., and Kim, Y. (2010). Challenges for rechargeable Li batteries. Chem. Mater. *22*, 587–603.

13. Choudhury, S., Wei, S., Ozhabes, Y., Gunceler, D., Zachman, M.J., Tu, Z., Shin, J.H., Nath, P., Agrawal, A., Kourkoutis, L.F., et al. (2017). Designing solid-liquid interphases for sodium batteries. Nat. Commun. *8*, 898.

14. Chazalviel, J. (1990). Electrochemical aspects of the generation of ramified metallic electrodeposits. Phys. Rev. A *42*, 7355–7367.

15. Bommier, C., and Ji, X. (2018). Electrolytes, SEI formation, and binders: a review of nonelectrode factors for sodium-ion battery anodes. Small *14*, 1703576.

16. Wood, S.M., Pham, C.H., Rodriguez, R., Nathan, S.S., Dolocan, A.D., Celio, H., Souza, J.P., Klavetter, K.C., Heller, A., and Mullins, C.B. (2016). K^+ reduces lithium dendrite growth by forming a thin, less-resistive solid electrolyte interphase. ACS Energy Lett. *1*, 414–419.

17. Cheng, X.B., Zhang, R., Zhao, C.Z., Wei, F., Zhang, J.G., and Zhang, Q. (2016). A review of solid electrolyte interphases on lithium metal anode. Adv. Sci. *3*, 1500213.

18. Leung, K., Soto, F., Hankins, K., Balbuena, P.B., and Harrison, K.L. (2016). Stability of solid electrolyte interphase components on lithium metal and reactive anode material surfaces. J. Phys. Chem. C *120*, 6302–6313.

19. Seh, Z.W., Sun, J., Sun, Y., and Cui, Y. (2015). A highly reversible room-temperature sodium metal anode. ACS Cent. Sci. *1*, 449–455.

20. Lv, D., Shao, Y., Lozano, T., Bennett, W.D., Graff, G.L., Polzin, B., Zhang, J., Engelhard, M.H., Saenz, N.T., Henderson, W.A., et al. (2015). Failure mechanism for fast-charged lithium metal batteries with liquid electrolytes. Adv. Energy Mater. *5*, 1400993.

21. Zheng, G., Lee, S.W., Liang, Z., Lee, H.W., Yan, K., Yao, H., Wang, H., Li, W., Chu, S., and Cui, Y. (2014). Interconnected hollow carbon nanospheres for stable lithium metal anodes. Nat. Nanotechnol. *9*, 618–623.

22. Liu, S., Xia, X., Zhong, Y., Deng, S., Yao, Z., Zhang, L., Cheng, X.-B., Wang, X., Zhang, Q., and Tu, J. (2017). 3D TiC/C core/shell nanowire skeleton for dendrite-free and long-life lithium metal anode. Adv. Energy Mater. *8*, 1702322.

23. Liang, Z., Zheng, G., Liu, C., Liu, N., Li, W., Yan, K., Yao, H., Hsu, P.C., Chu, S., and Cui, Y. (2015). Polymer nanofiber-guided uniform lithium deposition for battery electrodes. Nano Lett. *15*, 2910–2916.

24. Jäckle, M., and Groß, A. (2014). Microscopic properties of lithium, sodium, and magnesium battery anode materials related to possible dendrite growth. J. Chem. Phys. *141*, 174710.

25. Pang, Q., Liang, X., Shyamsunder, A., and Nazar, L.F. (2017). An *in vivo*, formed solid electrolyte surface layer enables stable plating of li metal. Joule *1*, 871–886.

26. Monroe, C., and Newman, J. (2003). Dendrite growth in Lithium/polymer systems. J. Electrochem. Soc. *150*, A1377–A1384.

27. Han, M., Zhu, C., Ma, T., Pan, Z., Tao, Z., and Chen, J. (2018). *In situ* atomic force microscopy study of nano-micro sodium deposition in ester-based electrolytes. Chem. Commun. (Camb.) *54*, 2381–2384.

28. Hong, Y.S., Li, N., Chen, H., Wang, P., Song, W.L., and Fang, D. (2017). In operando observation of chemical and mechanical stability of Li and Na dendrites under quasi-zero electrochemical field. Energy Storage Mater. *11*, 118–126.

29. Wood, K., Kazyak, E., Chadwick, A.F., Chen, K.H., Zhang, J.G., Thornton, K., and Dasgupta, N. (2016). Dendrites and pits: untangling the complex behavior of lithium metal anodes through operando video microscopy. ACS Cent. Sci. *2*, 790–801.

30. Wei, S., Choudhury, S., Xu, J., Nath, P., Tu, Z., and Archer, L.A. (2016). Highly stable sodium batteries enabled by functional ionic polymer membranes. Adv. Mater. *29*, 1605512.

31. Bhattacharyya, R., Key, B., Chen, H., Best, A.S., Hollenkamp, A.F., and Grey, C.P. (2010). *In situ* NMR observation of the formation of metallic lithium microstructures in lithium batteries. Nat. Mater. *9*, 504–510.

32. Bayley, P.M., Trease, N.M., and Grey, C.P. (2016). Insights into electrochemical sodium metal deposition as probed with *in situ* ^{23}Na NMR. J. Am. Chem. Soc. *138*, 1955–1961.

33. Li, L., Basu, S., Wang, Y., Chen, Z., Hundekar, P., Wang, B., Shi, J., Shi, Y., Narayanan, S., and Koratkar, N. (2018). Self-heating-induced healing of lithium dendrites. Science *359*, 1513–1516.

34. Wang, X., Zeng, W., Hong, L., Xu, W., Yang, H., Wang, F., Duan, H., Tang, M., and Jiang, H. (2018). Stress-driven lithium dendrite growth mechanism and dendrite mitigation by electroplating on soft substrates. Nat. Energy *3*, 227–235.

35. Kim, H., Jeong, G., Kim, Y.-U., Kim, J.-H., Park, C.-M., and Sohn, H.-J. (2013). Metallic anodes for next generation secondary batteries. Chem. Soc. Rev. *42*, 9011–9034.

36. Seong, I.W., Hong, C.H., Kim, B.K., and Yoon, W.Y. (2008). The effects of current density and amount of discharge on dendrite formation in the lithium powder anode electrode. J. Power Sources *178*, 769–773.

37. Ryou, M.-H., Lee, Y.M., Lee, Y., Winter, M., and Bieker, P. (2015). Mechanical surface modification of lithium metal: towards improved Li metal anode performance by directed Li plating. Adv. Funct. Mater. *25*, 834–841.

38. Raji, A.O., Villegas Salvatierra, R., Kim, N.D., Fan, X., Li, J.Y., Silva, G.A.L., Sha, J., and Tour, J.M. (2017). Lithium batteries with nearly maximum metal storage. ACS Nano *11*, 6362–6369.

39. Pei, A., Zheng, G., Shi, F., Li, Y., and Cui, Y. (2017). Nanoscale nucleation and growth of electrodeposited lithium metal. Nano Lett. *17*, 1132–1139.

40. Zhang, R., Chen, X.R., Chen, X., Cheng, X.B., Zhang, X.Q., Yan, C., and Zhang, Q. (2017). Lithiophilic sites in doped graphene guide uniform lithium nucleation for dendrite-free lithium metal anodes. Angew. Chem. Int. Ed. *56*, 7764–7768.

41. Mukherjee, R., Thomas, A.V., Datta, D., Singh, E., Li, J., Eksik, O., Shenoy, V.B., and Koratkar, N. (2014). Defect-induced plating of lithium metal within porous graphene networks. Nat. Commun. *5*, 3710.

42. Lin, D., Liu, Y., Liang, Z., Lee, H.W., Sun, J., Wang, H., Yan, K., Xie, J., and Cui, Y. (2016).

Layered reduced graphene oxide with nanoscale interlayer gaps as a stable host for lithium metal anodes. Nat. Nanotechnol. *11*, 626–632.

43. Cheng, X.B., Hou, T.Z., Zhang, R., Peng, H.J., Zhao, C.Z., Huang, J.Q., and Zhang, Q. (2016). Dendrite-free lithium deposition induced by uniformly distributed lithium ions for efficient lithium metal batteries. Adv. Mater. *28*, 2888–2895.

44. Liu, W., Lin, D., Pei, A., and Cui, Y. (2016). Stabilizing lithium metal anodes by uniform Li-ion flux distribution in nanochannel confinement. J. Am. Chem. Soc. *138*, 15443–15450.

45. Lin, D., Zhao, J., Sun, J., Yao, H., Liu, Y., Yan, K., and Cui, Y. (2017). Three-dimensional stable lithium metal anode with nanoscale lithium islands embedded in ionically conductive solid matrix. Proc. Natl. Acad. Sci. U S A *114*, 4613–4618.

46. Wang, A., Tang, S., Kong, D., Liu, S., Chiou, K., Zhi, L., Huang, J., Xia, Y.Y., and Luo, J. (2018). Bending-tolerant anodes for lithium-metal batteries. Adv. Mater. *30*, 1703891.

47. Wang, A., Hu, X., Tang, H., Zhang, C., Liu, S., Yang, Y.W., Yang, Q.H., and Luo, J. (2017). Processable and moldable sodium-metal anodes. Angew. Chem. Int. Ed. *56*, 11921–11926.

48. Yang, C.P., Yin, Y.X., Zhang, S.F., Li, N.W., and Guo, Y.G. (2015). Accommodating lithium into 3D current collectors with a submicron skeleton towards long-life lithium metal anodes. Nat. Commun. *6*, 8058.

49. Cohn, A.P., Muralidharan, N., Carter, R., Share, K., and Pint, C.L. (2017). Anode-free sodium battery through *in situ* plating of sodium metal. Nano Lett. *17*, 1296–1301.

50. Cao, R., Mishra, K., Li, X., Qian, J., Engelhard, M.H., Bowden, M.E., Han, K.S., Mueller, K.T., Henderson, W.A., and Zhang, J.-G. (2016). Enabling room temperature sodium metal batteries. Nano Energy *30*, 825–830.

51. Cheng, X.B., Yan, C., Chen, X., Guan, C., Huang, J.Q., Peng, H.J., Zhang, R., Yang, S.T., and Zhang, Q. (2017). Implantable solid electrolyte interphase in lithium-metal batteries. Chem *2*, 258–270.

52. Yan, K., Lee, H.W., Gao, T., Zheng, G., Yao, H., Wang, H., Lu, Z., Zhou, Y., Liang, Z., Liu, Z., et al. (2014). Ultrathin two-dimensional atomic crystals as stable interfacial layer for improvement of lithium metal anode. Nano Lett. *14*, 6016–6022.

53. Lee, Y.-G., Ryu, S., Sugimoto, T., Yu, T., Chang, W.-S., Yang, Y., Jung, C., Woo, J., Kang, S.G., Han, H.N., et al. (2017). Dendrite-free lithium deposition for lithium metal anodes with interconnected microsphere protection. Chem. Mater. *29*, 5906–5914.

54. Zhang, X.Q., Chen, X., Xu, R., Cheng, X.B., Peng, H.J., Zhang, R., Huang, J.Q., and Zhang, Q. (2017). Columnar lithium metal anodes. Angew. Chem. Int. Ed. *56*, 14207–14211.

55. Liang, X., Pang, Q., Kochetkov, I.R., Sempere, M.S., Huang, H., Sun, X., and Nazar, L.F. (2017). A facile surface chemistry route to a stabilized lithium metal anode. Nat. Energy *2*, 17119.

56. Tu, Z., Choudhury, S., Zachman, M.J., Wei, S., Zhang, K., Kourkoutis, L.F., and Archer, L.A. (2018). Fast ion transport at solid-solid interfaces in hybrid battery anodes. Nat. Energy *3*, 310–316.

57. Li, N.W., Yin, Y.X., Yang, C.P., and Guo, Y.G. (2016). An artificial solid electrolyte interphase layer for stable lithium metal anodes. Adv. Mater. *28*, 1853–1858.

58. Zhang, D., Li, B., Wang, S., and Yang, S. (2017). Simultaneous formation of artificial SEI film and 3D host for stable metallic sodium anodes. ACS Appl. Mater. Interfaces *9*, 40265–40272.

59. Luo, W., Lin, C.-F., Zhao, O., Noked, M., Zhang, Y., Rubloff, G.W., and Hu, L. (2017). Ultrathin surface coating enables the stable sodium metal anode. Adv. Energy Mater. *7*, 1601526.

60. Li, P.R., Xu, T.H., Ding, P., Deng, J., Zha, C.Y., Wu, Y.L., Wang, Y.Y., and Li, Y.G. (2018). Highly reversible Na and K metal anodes enabled by carbon paper protection. Energy Storage Mater. *15*, 8–13.

61. Zhu, B., Jin, Y., Hu, X., Zheng, Q., Zhang, S., Wang, Q., and Zhu, J. (2017). Poly(dimethylsiloxane) thin film as a stable interfacial layer for high-performance lithium-metal battery anodes. Adv. Mater. *29*, 1603755.

62. Liu, Y., Lin, D., Yuen, P.Y., Liu, K., Xie, J., Dauskardt, R.H., and Cui, Y. (2017). An artificial solid electrolyte interphase with high Li-ion conductivity, mechanical strength, and flexibility for stable lithium metal anodes. Adv. Mater. *29*, 1605531.

63. Sun, F., Zielke, L., Markötter, H., Hilger, A., Zhou, D., Moroni, R., Zengerle, R., Thiele, S., Banhart, J., and Manke, I. (2016). Morphological evolution of electrochemically plated/stripped lithium microstructures investigated by synchrotron X-ray phase contrast tomography. ACS Nano *10*, 7990–7997.

64. Ryou, M.-H., Lee, D.J., Lee, J.-N., Lee, Y.M., Park, J.-K., and Choi, J.W. (2012). Excellent cycle life of lithium-metal anodes in lithium-ion batteries with mussel-inspired polydopamine-coated separators. Adv. Energy Mater. *2*, 645–650.

65. Luo, W., Zhou, L., Fu, K., Yang, Z., Wan, J., Manno, M., Yao, Y., Zhu, H., Yang, B., and Hu, L. (2015). A thermally conductive separator for stable Li metal anodes. Nano Lett. *15*, 6149–6154.

66. Wu, H., Zhuo, D., Kong, D., and Cui, Y. (2014). Improving battery safety by early detection of internal shorting with a bifunctional separator. Nat. Commun. *5*, 5193.

67. Liu, K., Zhuo, D., Lee, H.-W., Liu, W., Lin, D., Lu, Y., and Cui, Y. (2017). Extending the life of lithium-based rechargeable batteries by reaction of lithium dendrites with a novel silica nanoparticle sandwiched separator. Adv. Mater. *29*, 1603987.

68. Chi, M., Shi, L., Wang, Z., Zhu, J., Mao, X., Zhao, Y., Zhang, M., Sun, L., and Yuan, S. (2016). Excellent rate capability and cycle life of Li metal batteries with ZrO_2/POSS multilayer-assembled PE separators. Nano Energy *28*, 1–11.

69. Hao, X., Zhu, J., Jiang, X., Wu, H., Qiao, J., Sun, W., Wang, Z., and Sun, K. (2016). Ultrastrong polyoxyzole nanofiber membranes for dendrite-proof and heat-resistant battery separators. Nano Lett. *16*, 2981–2987.

70. Ansari, Y., Guo, B., Cho, J.H., Park, K., Song, J., Ellison, C.J., and Goodenough, J.B. (2014). Low-cost, dendrite-blocking polymer-Sb_2O_3 separators for lithium and sodium batteries. J. Electrochem. Soc. *161*, A1655–A1661.

71. Ye, M., Xiao, Y., Cheng, Z., Cui, L., Jiang, L., and Qu, L. (2018). A smart, anti-piercing and eliminating-dendrite lithium metal battery. Nano Energy *49*, 403–410.

72. Yu, B.-C., Park, K., Jang, J.-H., and Goodenough, J.B. (2016). Cellulose-based porous membrane for suppressing Li dendrite formation in lithium-sulfur battery. ACS Energy Lett. *1*, 633–637.

73. Xu, J.-J., Liu, Q.-C., Yu, Y., Wang, J., Yan, J.-M., and Zhang, X.-B. (2017). *In situ* construction of stable tissue-directed/reinforced bifunctional separator/protection film on lithium anode for lithium-oxygen batteries. Adv. Mater. *29*, 1606552.

74. Qian, J., Henderson, W.A., Xu, W., Bhattacharya, P., Engelhard, M., Borodin, O., and Zhang, J.G. (2015). High rate and stable cycling of lithium metal anode. Nat. Commun. *6*, 6362.

75. Xiong, S., Xie, K., Diao, Y., and Hong, X. (2014). Characterization of the solid electrolyte interphase on lithium anode for preventing the shuttle mechanism in lithium-sulfur batteries. J. Power Sources *246*, 840–845.

76. Ding, F., Xu, W., Graff, G.L., Zhang, J., Sushko, M.L., Chen, X., Shao, Y., Engelhard, M.H., Nie, Z., Xiao, J., et al. (2013). Dendrite-free lithium deposition *via* self-healing electrostatic shield mechanism. J. Am. Chem. Soc. *135*, 4450–4456.

77. Xu, K., Lam, Y., Zhang, S.S., Jow, T.R., and Curtis, T.B. (2007). Solvation sheath of Li^+ in nonaqueous electrolytes and its implication of graphite/electrolyte interface chemistry. J. Phys. Chem. C *111*, 7411–7421.

78. Xu, K., Cresce, A.V., and Lee, U. (2010). Differentiating contributions to "ion transfer" barrier from interphasial resistance and Li desolvation at electrolyte/graphite interface. Langmuir *26*, 11538–11543.

79. Shi, S., Lu, P., Liu, Z., Qi, Y., Hector, L.G., Li, H., and Harris, S.J. (2012). Direct calculation of Li-ion transport in the solid electrolyte interphase. J. Am. Chem. Soc. *134*, 15476–15487.

80. Suo, L., Hu, Y.S., Li, H., Armand, M., and Chen, L. (2013). A new class of solvent-in-salt electrolyte for high-energy rechargeable metallic lithium batteries. Nat. Commun. *4*, 1481.

81. Chen, S., Zheng, J., Mei, D., Han, K.S., Engelhard, M.H., Zhao, W., Xu, W., Liu, J., and

Zhang, J.G. (2018). High-voltage lithium-metal batteries enabled by localized high-concentration electrolytes. Adv. Mater. *30*, e1706102.

82. Li, S., Jiang, M.W., Xie, Y., Xu, H., Jia, J.Y., and Li, J. (2018). Developing high-performance lithium metal anodes in liquid electrolytes: challenges and progress. Adv. Mater. *30*, 1706735.

83. Zhang, X.-Q., Cheng, X.-B., Chen, X., Yan, C., and Zhang, Q. (2017). Fluoroethylene carbonate additives to render uniform Li deposits in lithium metal batteries. Adv. Funct. Mater. *27*, 1605989.

84. Zhang, X.Q., Chen, X., Cheng, X.B., Li, B.Q., Shen, X., Yan, C., Huang, J.Q., and Zhang, Q. (2018). Highly stable lithium metal batteries enabled by regulating the Li^+ solvation in nonaqueous electrolyte. Angew. Chem. Int. Ed. *130*, 5399–5403.

85. Lu, Y., Tu, Z., and Archer, L.A. (2014). Stable lithium electrodeposition in liquid and nanoporous solid electrolytes. Nat. Mater. *13*, 961–969.

86. Liu, Q.-C., Xu, J.-J., Yuan, S., Chang, Z.-W., Xu, D., Yin, Y.-B., Li, L., Zhong, H.-X., Jiang, Y.-S., Yan, J.-M., and Zhang, X.-B. (2015). Artificial protection film on lithium metal anode toward long-cycle-life lithium-oxygen batteries. Adv. Mater. *27*, 5241–5247.

87. Dugas, R., Ponrouch, A., Gachot, G., David, R., Palacin, M.R., and Tarascon, J.M. (2016). Na reactivity toward carbonate-based electrolytes: the effect of FEC as additive. J. Electrochem. Soc. *163*, A2333–A2339.

88. Zhang, W.C., Pang, W.K., Sencadas, V., and Guo, Z.P. (2018). Understanding high-energy-density Sn_4P_3 anodes for potassium-ion batteries. Joule *2*, 1–14.

89. Li, W., Yao, H., Yan, K., Zheng, G., Liang, Z., Chiang, Y.M., and Cui, Y. (2015). The synergetic effect of lithium polysulfide and lithium nitrate to prevent lithium dendrite growth. Nat. Commun. *6*, 7436.

90. Wang, H., Wang, C., Matios, E., and Li, W. (2018). Facile stabilization of sodium metal anode with additives: unexpected key role of sodium polysulfide and adverse effect of sodium nitrate. Angew. Chem. Int. Ed. *130*, 7860–7863.

91. Yoo, D.J., Kim, K.J., and Choi, J.W. (2018). The synergistic effect of cation and anion of an ionic liquid additive for lithium metal anodes. Adv. Energy Mater. *8*, 1702744.

92. Yu, S., and Siegel, D.J. (2018). Grain boundary contributions to Li-ion transport in the solid electrolyte $Li_7La_3Zr_2O_{12}$ (LLZO). Chem. Mater. *29*, 9639–9647.

93. Tsai, C.L., Roddatis, V., Chandran, C.V., Ma, Q., Uhlenbruck, S., Bram, M., Heitjans, P., and Guillon, O. (2016). $Li_7La_3Zr_2O_{12}$ interface modification for Li dendrite prevention. ACS Appl. Mater. Interfaces *8*, 10617–10626.

94. Ren, Y., Shen, Y., Lin, Y., and Nan, C.W. (2015). Direct observation of lithium dendrites inside garnet-type lithium-ion solid electrolyte. Electrochem. Commun. *57*, 27–30.

95. Nagao, M., Hayashi, A., Tatsumisago, M., Kanetsuku, T., Tsuda, T., and Kuwabata, S. (2013). *In situ* SEM study of a lithium deposition and dissolution mechanism in a bulk-type solid-state cell with a Li_2S-P_2S_5 solid electrolyte. Phys. Chem. Chem. Phys. *15*, 18600–18606.

96. Zhou, W., Li, Y., Xin, S., and Goodenough, J.B. (2017). Rechargeable sodium all-solid-state battery. ACS Cent. Sci. *3*, 52–57.

97. Han, X., Gong, Y., Fu, K.K., He, X., Hitz, G.T., Dai, J., Pearse, A., Liu, B., Wang, H., Rubloff, G., et al. (2017). Negating interfacial impedance in garnet-based solid-state Li metal batteries. Nat. Mater. *16*, 572–579.

98. Fu, K., Gong, Y., Dai, J., Gong, A., Han, X., Yao, Y., Wang, C., Wang, Y., Chen, Y., Yan, C., et al. (2016). Flexible, solid-state, ion-conducting membrane with 3D garnet nanofiber networks for lithium batteries. Proc. Natl. Acad. Sci. U S A *113*, 7094–7099.

99. Zhou, W., Wang, S., Li, Y., Xin, S., Manthiram, A., and Goodenough, J.B. (2016). Plating a dendrite-free lithium anode with a polymer/ceramic/polymer sandwich electrolyte. J. Am. Chem. Soc. *138*, 9385–9388.

100. Khurana, R., Schaefer, J.L., Archer, L.A., and Coates, G.W. (2014). Suppression of lithium dendrite growth using cross-linked polyethylene/poly(ethylene oxide) electrolytes: a new approach for practical lithium-metal polymer batteries. J. Am. Chem. Soc. *136*, 7395–7402.

101. Lin, D., Liu, W., Liu, Y., Lee, H.R., Hsu, P.C., Liu, K., and Cui, Y. (2016). High ionic conductivity of composite solid polymer electrolyte *via in situ* synthesis of monodispersed SiO_2 nanospheres in poly(ethylene oxide). Nano Lett. *16*, 459–465.

102. Zhang, Z., Zhang, Q., Ren, C., Luo, F., Ma, Q., Hu, Y.-S., Zhou, Z., Li, H., Huang, X., and Chen, L. (2016). A ceramic/polymer composite solid electrolyte for sodium batteries. J. Mater. Chem. A *4*, 15823–15828.

103. Song, S., Kotobuki, M., Zheng, F., Xu, C., Savilov, S.V., Hu, N., Lu, L., Wang, Y., and Li, W.D.Z. (2017). A hybrid polymer/oxide/ionic-liquid solid electrolyte for Na-metal batteries. J. Mater. Chem. A *5*, 6424–6431.